22. Tabuchi Y, Ohta S, Arai Y, et al. Establishment and characterization of a colonic epithelial cell line MCE301 from transgenic mice harboring temperature-sensitive simian virus 40 large T-antigen gene. Cell Struct Funct 2000;25:297–307.
23. Dohi T, Rennert PD, Fujihashi K, et al. Elimination of colonic patches with lymphotoxin beta receptor-Ig prevents Th2 cell-type colitis. J Immunol 2001;167:2781–2790.
24. Girgenrath M, Weng S, Kostek CA, et al. TWEAK, via its receptor Fn14, is a novel regulator of mesenchymal progenitor cells and skeletal muscle regeneration. EMBO J 2006;25:5826–5839.
25. Papadakis KA. Chemokines in inflammatory bowel disease. Curr Allergy Asthma Rep 2004;4:83–89.
26. Kucharzik T, Maaser C, Lugering A, et al. Recent understanding of IBD pathogenesis: implications for future therapies. Inflamm Bowel Dis 2006;12:1068–1083.
27. Naito Y, Yoshikawa T. Role of matrix metalloproteinases in inflammatory bowel disease. Mol Aspects Med 2005;26:379–390.
28. Abreu MT, Fukata M, Arditi M. TLR signaling in the gut in health and disease. J Immunol 2005;174:4453–4460.
29. Kamata K, Kamijo S, Nakajima A, et al. Involvement of TNF-like weak inducer of apoptosis in the pathogenesis of collagen-induced arthritis. J Immunol 2006;177:6433–6439.
30. Perper SJ, Browning B, Burkly LC, et al. TWEAK is a novel arthritogenic mediator. J Immunol 2006;177:2610–2620.
31. Arihiro S, Ohtani H, Hiwatashi N, et al. Vascular smooth muscle cells and pericytes express MMP-1, MMP-9, TIMP-1 and type I procollagen in inflammatory bowel disease. Histopathology 2001;39:50–59.
32. Pender SL, Fell JM, Chamow SM, et al. A p55 TNF receptor immunoadhesin prevents T cell-mediated intestinal injury by inhibiting matrix metalloproteinase production. J Immunol 1998; 160:4098–4103.
33. Di Sebastiano P, di Mola FF, Artese L, et al. Beneficial effects of Batimastat (BB-94), a matrix metalloproteinase inhibitor, in rat experimental colitis. Digestion 2001;63:234–239.
34. Sykes AP, Bhogal R, Brampton C, et al. The effect of an inhibitor of matrix metalloproteinases on colonic inflammation in a trinitrobenzenesulphonic acid rat model of inflammatory bowel disease. Aliment Pharmacol Ther 1999;13:1535–1542.
35. Targan SR, Hanauer SB, van Deventer SJ, et al. A short-term study of chimeric monoclonal antibody cA2 to tumor necrosis factor alpha for Crohn's disease. Crohn's Disease cA2 Study Group. N Engl J Med 1997;337:1029–1035.
36. Rutgeerts P, Sandborn WJ, Feagan BG, et al. Infliximab for induction and maintenance therapy for ulcerative colitis. N Engl J Med 2005;353:2462–2476.

Received March 25, 2008. Accepted November 6, 2008.

Reprint requests

Address requests for reprints to: Linda C. Burkly, PhD, Biogen Idec, 12 Cambridge Center, Cambridge, Massachusetts 02142. e-mail: linda.burkly@biogenidec.com; fax: (617) 679-3148.

Conflicts of interest

The authors disclose no conflicts.

Funding

Supported by Biogen Idec, Inc, and grants and contracts from the Ministry of Health, Labor, and Welfare, the program Grants-in-Aid for Scientific Research from the Ministry of Education, Cultures, Sports, Science, and Technology, and the Japan Health Sciences Foundation and Organization.

Supplementary Methods

Cell Subsets Analysis for WT and TWEAK KO Mice

TWEAK KO and WT mouse splenocytes were stained using antibodies (BD Biosciences) for CD3, CD4, CD8, IgM, NK1.1, DX5, CD44, and CD62L.

Immunohistochemistry

Fixed-frozen colon sections were blocked with human IgG (10 ìg/mL) for 15 minutes, treated with BlockAce for 30 minutes at room temperature, blocked with Avidin-biotin blocking kit and then incubated with biotinylated anti-TWEAK mAb (huP2D10) (1.5 ìg/mL in 0.2% BlockAce) for 1 hour at room temperature, followed by Streptavidin-Alexa488 (1:500 dilution, 30 minutes). Serial sections were stained with PE-labeled anti-epithelial cell adhesion molecule (anti-EpCAM) mAb (eBiosicence, San Diego, CA; 1:3000). Fn14 detection was carried out as described in the Methods section with double staining for PE-labeled EpCAM mAb as above or PE-labeled anti-F4/80 (Becton, Dickinson and Company, Franklin Lakes, NJ; 1:200 dilution) for 2 hours at room temperature. To visualize proliferating cells after 3-Gy ã-irradiation, 1 mg bromodeoxyuridine (BrdU) was injected intraperitoneally 1 hour before the mice were killed, jejuna were collected at 24 hours postirradiation, and paraffin-embedded sections were deparaffinized, treated with 4N HCl, blocked with 1% bovine serum albumin and stained with rat anti-BrdU antibody (Oxford Biotech, Ltd, United Kingdom), followed by fluorescein isothiocyanate-labeled anti-rat IgG (Southern Biotechnology Associates, Inc). Numbers of $BrdU^+$ cells were counted in 20 separate crypts in 3 or more fields for each animal.

Histologic Scoring System for Cell Infiltration

The colons of surviving mice were cut into proximal, middle and distal segments. Tissues were formalin-fixed and paraffin-embedded, and 4-μm sections were stained with H&E. Each colon segment was scored individually, and these scores were summed to reach a total score for the entire colon. The overall magnitude of inflammatory cell infiltration was scored for each colon segment as follows: no infiltration, 0; mild infiltration, 1; severe infiltration, 2. Thus, the total possible cell infiltration score is 6.

Gene Expression Profiling and Analysis

Sample labeling, hybridization, and scanning were carried out according to the Eukaryotic Target Preparation protocol in the Affymetrix Technical Manual for Genechip Expression Analysis (Affymetrix). The complementary RNA product was purified, fragmented, and applied to a Mouse Genome Mouse 430 2.0 GeneChip probe array representing more than 45,000 transcripts and transcript variants. The percent of genes called present, an indicator of sample quality, was determined using Microarray Suite 5.0 probe reduction algorithms. Analyses were performed using BRB-ArrayTools developed by Dr. Richard Simon and the BRB-ArrayTools Development Team (National Cancer Institute, Bethesda, MD).[1,2] Comparisons between groups used a random-variance t test to generate P values.[3] We controlled for false positives by limiting our lists based on the multivariate permutation test.[4] We specified a 90% confidence that the false discovery rate within each list is less than 10%. Fold changes were generated using the log2 average intensity for each group of samples.

Stimulation of Primary Colon Tissue Cultures

Balb/c colons were taken, and 1-cm-length opened segments were cultured as previously described[5] for 6 hours with media alone, a synthetic oligodeoxynucleotide containing CpG motifs, CpG ODN 1688 (Invivogen, San Diego, CA), which mimics bacterial DNA, or TNFα (R&D Systems, Minneapolis, MN), with segments from 3 individual mice per treatment group. Fn14 RNA levels were quantified by real-time polymerase chain reaction and normalized to glyceraldehyde-3-phosphate dehydrogenase (GAPDH) RNA levels as described.[6] Fn14 expression is shown as relative expression to the mean value for cultures with media alone.

References

1. Gautier L, Cope L, Bolstad BM, et al. affy–analysis of Affymetrix GeneChip data at the probe level. Bioinformatics 2004;20:307–315.
2. Gentleman RC, Carey VJ, Bates DM, et al. Bioconductor: open software development for computational biology and bioinformatics. Genome Biol 2004;5:R80.
3. Wright GW, Simon RM. A random variance model for detection of differential gene expression in small microarray experiments. Bioinformatics 2003;19:2448–2455.
4. Korn EL, Troendle JF, McShane LM, et al. Controlling the number of false discoveries: application to high-dimensional genomic data. J Stat Plan Inference 2004;124:379–398.
5. Kawashima R, Kawamura YI, Kato R, et al. IL-13 receptor alpha2 promotes epithelial cell regeneration from radiation-induced small intestinal injury in mice. Gastroenterology 2006; 131:130–141.
6. Jakubowski A, Ambrose C, Parr M, et al. TWEAK induces liver progenitor cell proliferation. J Clin Invest 2005;115:2330–2340.

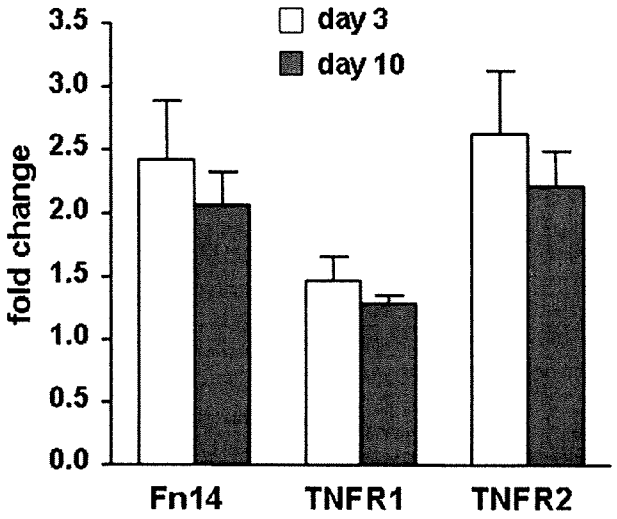

Supplementary Figure 1. mRNA expression of TNFR family members in TNBS colitis by gene chip analysis. Fold change in mean expression intensity compared with untreated control Balb/c mice; n = 3 for untreated, and n = 6 animals for day 3 (*white bars*) and 5 animals for day 10 (*gray bars*) TNBS-treated mice. $P < .01$ for all treated versus untreated comparisons. *Error bars* are SEM.

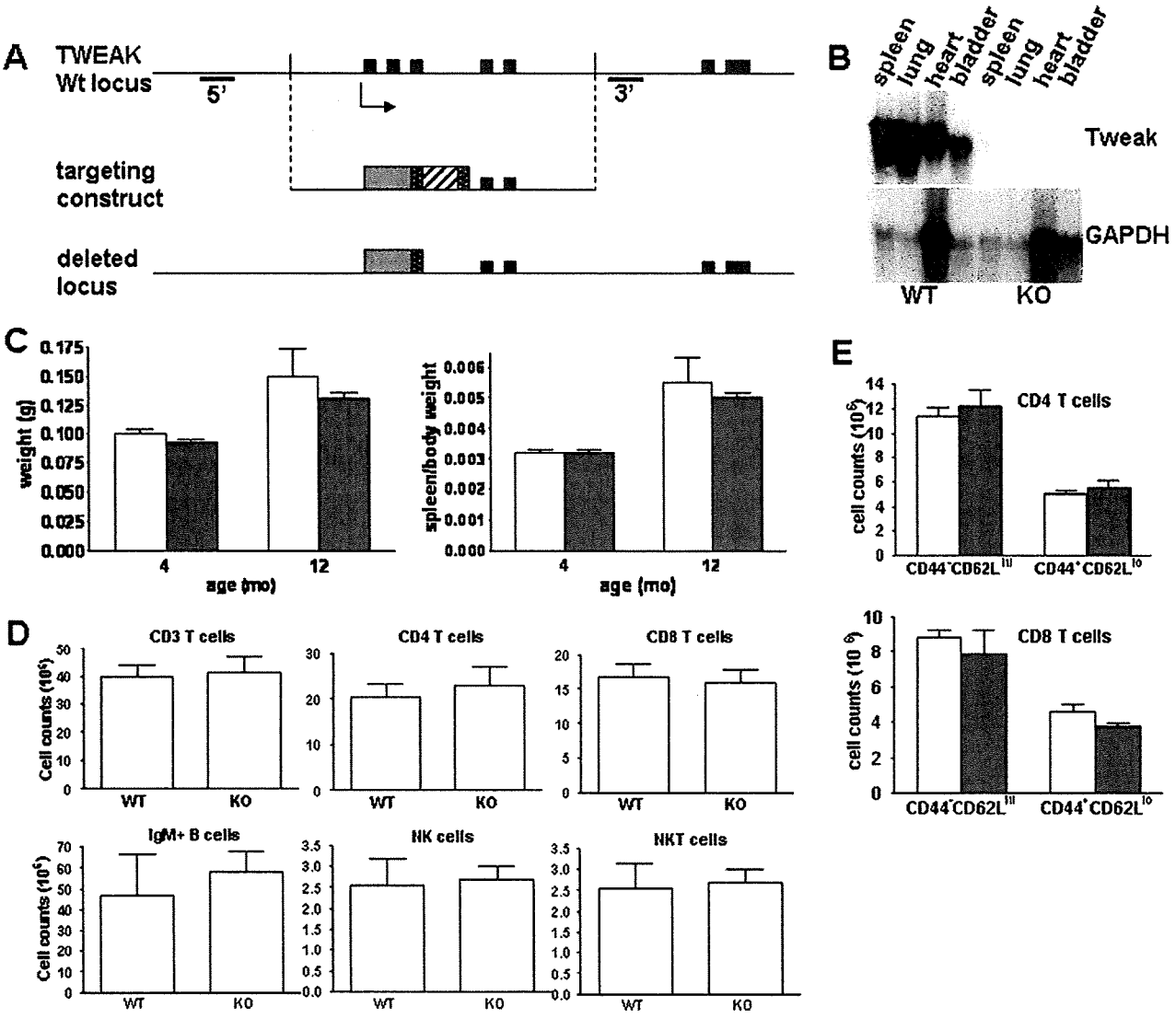

Supplementary Figure 2. TWEAK KO mice, generation and immune system analysis. (*A*) The genomic loci for TWEAK WT and KO; WT locus, neomycin-containing targeting construct, neo-deleted locus. The coding exons are shown as *black boxes*. *Arrow* indicates direction of transcription. The targeting construct contains a human CD2 expression cassette (*gray box*) and a loxP-flanked neomycin cassette (*striped box flanked by solid black*). In the neo-deleted TWEAK KO locus, the CD2 cassette and one loxP element remain. Bold lines (5' and 3') beneath the WT genomic locus mark the positions of external Southern blot probes. (*B*) Northern blot analysis of tissues from TWEAK KO and WT mice. Fifteen micrograms of RNA from the indicated tissues was probed for GAPDH or TWEAK, using the full-length TWEAK complementary DNA. (*C*) Spleen weight and spleen weight–to–body weight ratio for 4- or 12-month-old TWEAK KO and WT mice (WT, *open bars*; KO, *filled bars*). (*D*) Immune cell subsets from the spleens of TWEAK KO and WT mice. Numbers of cells belonging to the indicated subsets are plotted. Four-month-old mice were used to measure NK and NKT cells; 12-month-old mice were used for all other analyses. (*E*) Levels of activated/memory cells within the CD4 and CD8 spleen T-cell populations from 12-month-old animals. All *error bars* are SEM; 5–7 mice per group were used for the comparisons; no significant differences.

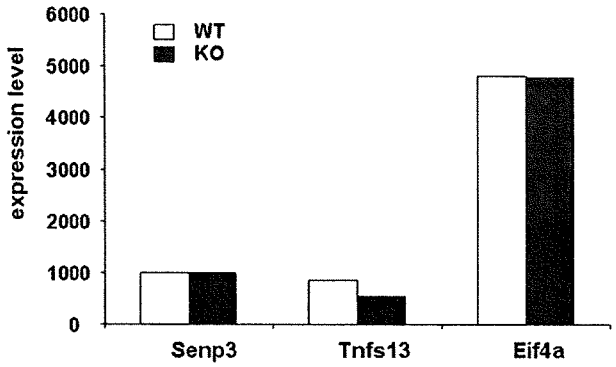

Supplementary Figure 3. mRNA expression of TWEAK locus neighbors *Senp3 (SMT3IP1)*, *Tnfs13 (APRIL)*, and *Eif4a* by gene array analysis of colon tissue from TWEAK KO and WT Balb/c mice. Averages for 3 animals per group are plotted, with no significant differences.

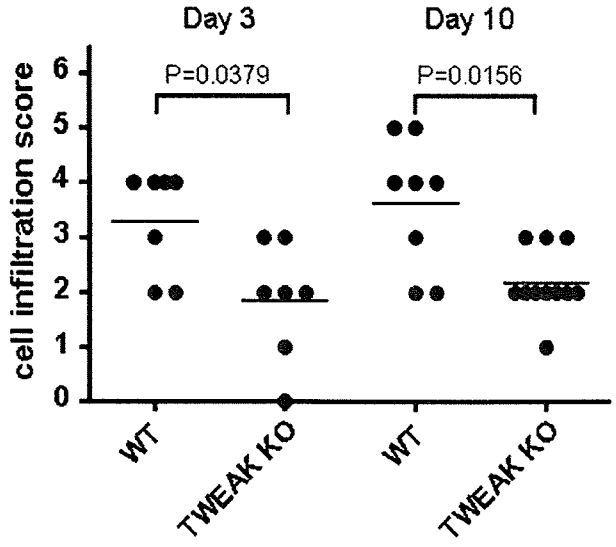

Supplementary Figure 4. Inflammatory cell infiltrations scores for TNBS colitis in Balb/c WT and TWEAK KO mice on day 3 (n = 7 per group) and day 10 (WT, n = 8; KO, n = 11). Mean values (*horizontal lines*) and *P* values by Mann-Whitney test are shown.

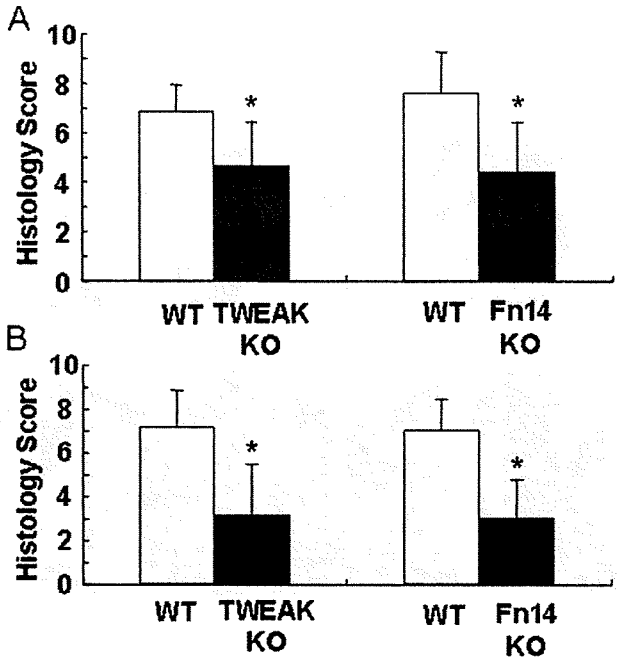

Supplementary Figure 5. Histologic scores for TNBS colitis in TWEAK KO, Fn14 KO, and WT mice on the C57BL/6 background. (*A*) Scores on day 3 of the colitis protocol. (*B*) Scores on day 10 of the colitis protocol. All differences are significant; $P < .05$ by the Mann-Whitney test.

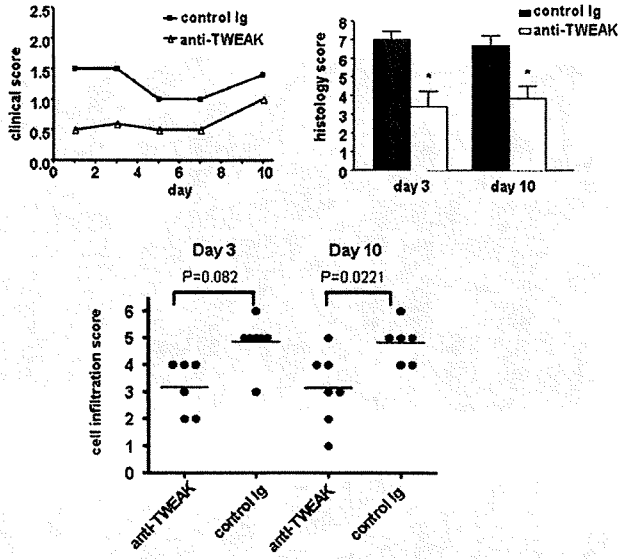

Supplementary Figure 6. Mean clinical scores in Balb/c mice treated with anti-TWEAK mAb or control Ig (n = 8 per group) starting on day 0. Mice killed on day 3 received 300 μg of Ab intraperitoneally on day 0, and mice killed on day 10 received 300 μg on days 0, 3, and 7. Difference between the groups was statistically significant by 2-way ANOVA, $P = 0.049$. Mean histologic scores ± SEM for colons of surviving mice treated with anti-TWEAK antibody or control Ig starting on day 0 relative to TNBS administration and killed on day 3 (anti-TWEAK, n = 12; control Ig treated, n = 15) or day 10 (anti-TWEAK, n = 7; control Ig treated, n = 6). *Asterisks* indicate significant *P* values by Mann-Whitney test; $P = .0025$ for day 3, $P = .0184$ for day 10. Inflammatory cell infiltrations score on day 3 and day 10 (n = 6–7 per group). Mean values (*horizontal lines*) and *P* values by Mann-Whitney test are shown.

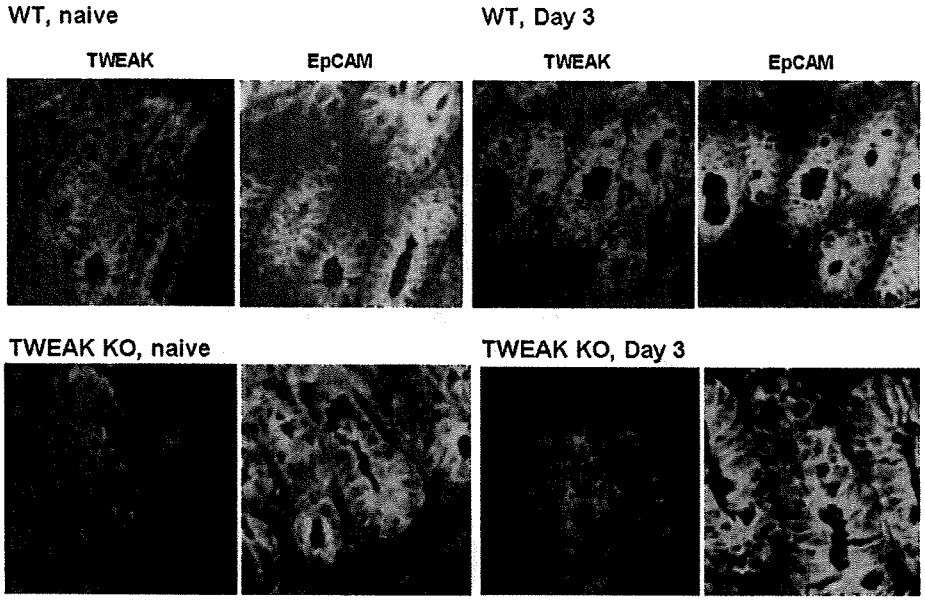

Supplementary Figure 7. TWEAK is expressed by colon epithelial cells. Representative images of single staining with anti-TWEAK (*green*) and epithelial marker EpCAM (*red*) on serial colon sections from Balb/c WT and TWEAK KO mice, naïve or 3 days after TNBS colitis. Anti-TWEAK staining of TWEAK KO serves as a control and reflects a low level of nonspecific staining.

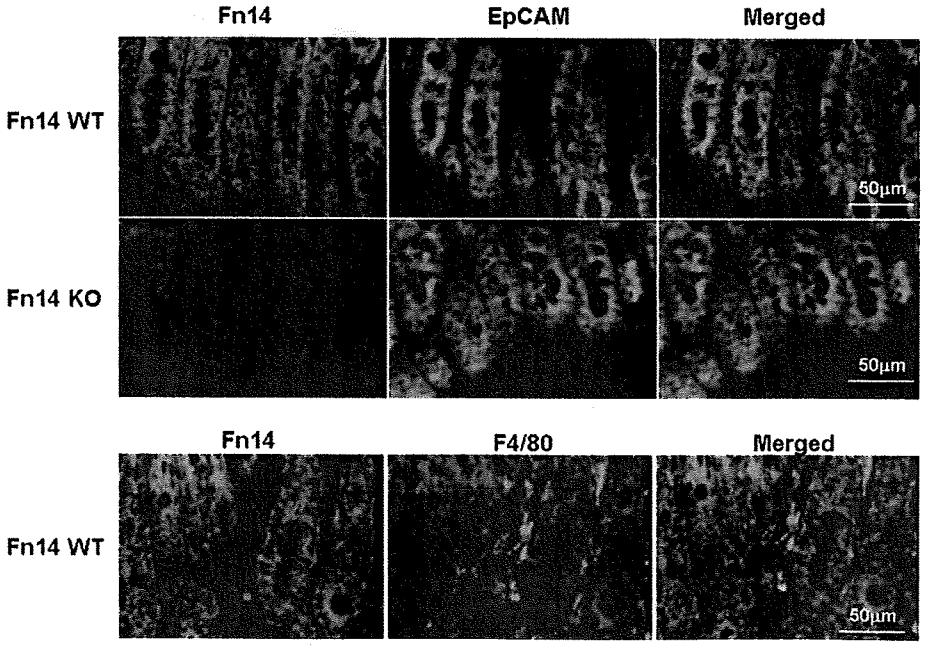

Supplementary Figure 8. Fn14 is expressed by colon epithelial cells and not infiltrating macrophages. Representative images of anti-Fn14 (*green*) double staining with epithelial marker EpCAM (*red*) or macrophage marker F4/80 (*red*) on colon sections from WT and Fn14 KO mice 3 days after TNBS colitis.

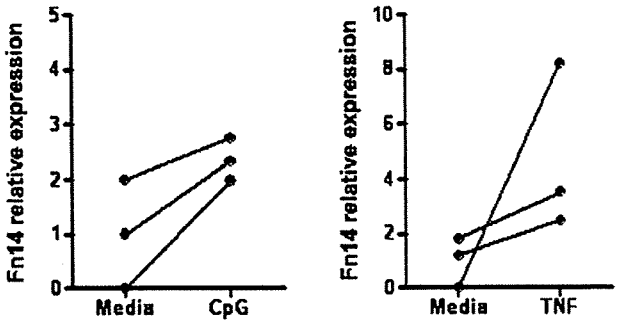

Supplementary Figure 9. Fn14 mRNA expression is up-regulated by CpG ODN or TNFα. Fn14 relative expression values for primary colon tissue cultures with media or stimuli as shown. Each line represents a culture from an individual mouse.

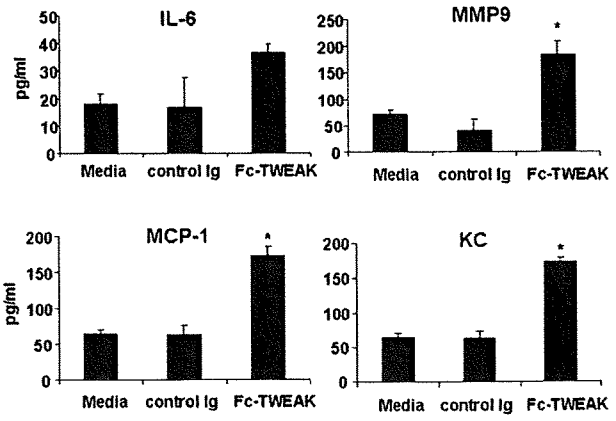

Supplementary Figure 10. TWEAK-induced colon epithelial cell production of inflammatory mediators. IL-6, MMP-9, MCP-1, and KC production by the colon epithelial cell MCE301 cultured in the presence of 100 ng/mL Fc-TWEAK, control Ig, or without stimulation (media). Differences between Fc-TWEAK and media are significant for each mediator. $P < .01$ by Student two-tailed t test. *Asterisks* indicate that differences between Fc-TWEAK and control Ig are significant for MMP-9 ($P = 0.008$), MCP-1 ($P = 0.001$), and KC ($P = 0.03$).

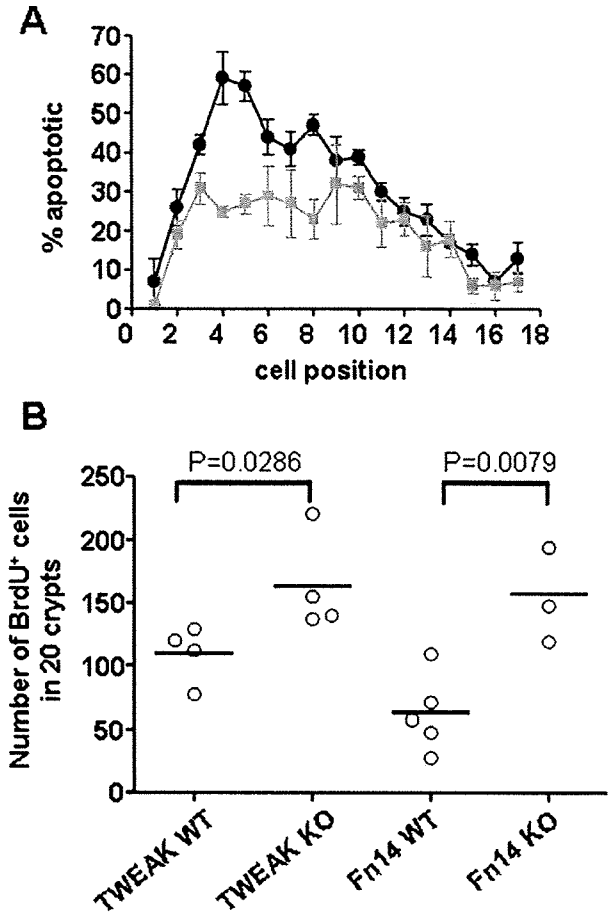

Supplementary Figure 11. (*A*) Percentage of apoptotic cells at various crypt positions for C57BL/6 WT (*black*) versus Fn14 KO (*red*) jejunum after 3-Gy γ-irradiation, plotted as mean values ± SEM (n = 5 per group). Significant differences by Student two-tailed *t* test ($P < .05$) between KO and WT animals were observed at positions 3, 4, and 5. (*B*) Number of proliferating ($BrdU^+$) cells per crypt in the jejunum after whole-body irradiation of Balb/c WT and TWEAK KO mice (n = 4 per group) and C57BL/6 WT and Fn14 KO mice (n = 5 per group). *P* values shown as determined by Student two-tailed *t* test.

Inhibition of CCL1-CCR8 Interaction Prevents Aggregation of Macrophages and Development of Peritoneal Adhesions[1]

Akiyoshi Hoshino,* Yuki I. Kawamura,[†¶] Masato Yasuhara,[§] Noriko Toyama-Sorimachi,[†] Kenji Yamamoto,[‡] Akihiro Matsukawa,[‖] Sergio A. Lira,[#] and Taeko Dohi[2†]

Peritoneal adhesions are a significant complication of surgery and visceral inflammation; however, the mechanism has not been fully elucidated. The aim of this study was to clarify the mechanism of peritoneal adhesions by focusing on the cell trafficking and immune system in the peritoneal cavity. We investigated the specific recruitment of peritoneal macrophages (PMϕ) and their expression of chemokine receptors in murine models of postoperative and postinflammatory peritoneal adhesions. PMϕ aggregated at the site of injured peritoneum in these murine models of peritoneal adhesions. The chemokine receptor CCR8 was up-regulated in the aggregating PMϕ when compared with naive PMϕ. The up-regulation of CCR8 was also observed in PMϕ, but not in bone marrow-derived Mϕ, treated with inflammatory stimulants including bacterial components and cytokines. Importantly, CCL1, the ligand for CCR8, a product of both PMϕ and peritoneal mesothelial cells (PMCs) following inflammatory stimulation, was a potent enhancer of CCR8 expression. Cell aggregation involving PMϕ and PMCs was induced in vitro in the presence of CCL1. CCL1 also up-regulated mRNA levels of plasminogen activator inhibitor-1 in both PMϕ and PMCs. *CCR8* gene-deficient mice or mice treated with anti-CCL1-neutralizing Ab exhibited significantly reduced postoperational peritoneal adhesion. Our study now establishes a unique autocrine activation system in PMϕ and the mechanism for recruitment of PMϕ together with PMCs via CCL1/CCR8, as immune responses of peritoneal cavity, which triggers peritoneal adhesions. *The Journal of Immunology,* 2007, 178: 5296–5304.

The serosal membrane of viscera and the peritoneal cavity are involved in numerous types of inflammation and surgical intervention. For example, in the case of surgery, postoperative adhesions occur in the majority of patients following laparotomy and laparoscopy (1, 2). Peritoneal adhesions cause significant signs and symptoms including intestinal obstruction, chronic pelvic pain and infertility, and eventually a second more serious surgery is often required. Thus, adhesions in the peritoneal cavity are both life-threatening and an enormous cost for patient care. For example, 34.6% of patients who had undergone intra-abdominal surgery were readmitted within the next 10 years for a disorder directly or possibly related to adhesions, or for abdominal or pelvic surgery that could be potentially complicated by adhesions (2). Despite the large number of surgical operations performed daily, the mechanism for peritoneal adhesions is not well-understood. Previous reports showed that peritoneal injury is triggered by leakage of plasma proteins, followed by formation of fibrinous deposits and proliferation of fibroblasts (3). A rapid and transient influx of neutrophils into the peritoneal cavity also occurs followed by an accumulation of mononuclear cells, largely macrophages (Mϕ)[3] (4, 5). CD4-positive T cells also play a significant role in peritoneal adhesions together with the T cell-derived proinflammatory cytokine, IL-17 (6), and the programmed death-1 inhibitory pathway (7). Although active roles for these cells in adhesions have been shown (8, 9), little is yet known about the cell origin or the dynamics of migration to help explain the peritoneal adhesion events. Inflammation such as appendicitis, endometriosis, and pelvic inflammatory disease can also cause peritoneal adhesion, which can lead to infertility and reproductive problems. In the case of Crohn's disease, intestinal transmural ulcerations with fissures or fistulas are the most important pathological findings (10). These Crohn's disease lesions involve the intestinal serosa and mesentery. The characteristic changes in the serosal surface, including fat wrapping, correlate directly with overall extent of inflammatory changes: the stricture of the intestine (10, 11), the depth of lymphoid aggregate penetration, and the number of lymphoid aggregates in the underlying ileal wall (12). These observations suggest that inflammation of viscera is not limited to the organ, but provokes responses in the peritoneal cavity as well. Most importantly, pathological changes in the peritoneal cavity cause serious symptoms and directly affect the quality of life of patients.

*Department of Medical Ecology and Informatics, [†]Department of Gastroenterology, and [‡]Research Institute, International Medical Center of Japan, Tokyo, Japan; [§]Department of Pharmacokinetics and Pharmacodynamics, Hospital Pharmacy, Tokyo Medical and Dental University Graduate School, Tokyo, Japan; [¶]G.S. Platz Company, Tokyo, Japan; [‖]Department of Pathology and Experimental Medicine, Graduate School of Medical, Dentistry, and Pharmaceutical Sciences, Okayama University, Okayama, Japan; and [#]Immunology Center, Mount Sinai School of Medicine, New York, NY 10029

Received for publication October 17, 2006. Accepted for publication January 23, 2007.

The costs of publication of this article were defrayed in part by the payment of page charges. This article must therefore be hereby marked *advertisement* in accordance with 18 U.S.C. Section 1734 solely to indicate this fact.

[1] This work was supported in part by Medical Techniques Promotion Research Grant H14-nano-004 from the Ministry of Health, Labor, and Welfare of Japan; grants and contracts from the Ministry of Health, Labor, and Welfare; the Ministry of Education, Culture, Sports, Science, and Technology; the Japan Health Sciences Foundation; and the Japan Science and Technology Agency.

[2] Address correspondence and reprint requests to Dr. Taeko Dohi, Department of Gastroenterology, Research Institute, International Medical Center of Japan, Toyama 1-21-1, Shinjuku, Tokyo 162-8655, Japan. E-mail address: dohi@ri.imcj.go.jp

[3] Abbreviations used in this paper: Mϕ, macrophage; BMϕ, bone marrow-derived Mϕ; PMϕ, peritoneal Mϕ; QD, quantum dot; PGN, peptidoglycan; pAb, polyclonal Ab; TNBS, 2,4,6-trinitrobenzene sulfonic acid; PTX, pertussis toxin; CIMA, chemokine-induced macrophage aggregation; PMC, peritoneal mesothelial cell; tPA, tissue-type plasminogen activator; PAI-1, plasminogen activator inhibitor-1.

Table I. *List of primers for RT-PCR*

	Forward	Reverse
CCR1	GTGTTCATCATTGGAGTGGTGG	GGTTGAACAGGTAGATGCTGGTC
CCR2	TGTTACCTCAGTTCATCCACGG	CAGAATGGTAATGTGAGCAGGAAG
CCR3	TTGCAGGACTGGCAGCATT	CCATAACGAGGAGAGGAAGAGCTA
CCR4	TCTACAGCGGCATCTTCTTCAT	CAGTACGTGTGGTTGTGCTCTG
CCR5	CATCGATTATGGTATGTCAGCACC	CAGAATGGTAGTGTGAGCAGGAA
CCR6	ACTCTTTGTCCTCACCCTACCG	ATCCTGCAGCTCGTATTTCTTG
CCR7	CATCAGCATTGACCGCTACGT	GGTACGGATGATAATGAGGTAGCA
CCR8	ACGTCACGATGACCGACTACTAC	GAGACCACCTTACACATCGCAG
CCR9	CCATTCTTGTAGTGCAGGCTGTT	AAGCTTCAAGCTACCCTCTCTCC
CCR10	AGAGCTCTGTTACAAGGCTGATGTC	CAGGTGGTACTTCCTAGATTCCAGC
CXCR1	TTGCACCAACCAAGGTATCAAG	GATGAAGAAGATGCCGCTGTAG
CXCR2	CATCTTATACAACCGGAGCACC	TAGTAACCACATGGCTATGCACAC
CXCR3	ATCAGGCGCTTCAATGCCAC	TGGCTTTCTCGACCACAGTT
CXCR4	TACATCTGTGACCGCCTTTACC	TCCACTTGTGCACGATGCT
CXCR5	TCCTACTACCGATGCTTGTGATG	ACGCCAGCGAAGGTGTAAA
CCL1	GCTGCCGTGTGGATACAGGA	GAATACCACAGCTGGGGGAT
tPA	CCAGACCGAGACTTGAAGCCC	ACACCCTTTCCCAACATAGCAG
PAI-1	ATCAATGACTGGGTGGAAAG	AGCCTGGTCATGTTGCCCTT
GAPDH	AGTATGACTCCACTCACGGCAA	TCTCGCTCCTGGAAGATGGT

However, the mechanism of peritoneal inflammation has not been fully understood at the cellular and molecular levels.

In this study, we postulated that there is a common serosal defense system that responds to both visceral inflammation and surgical stress. To clarify the molecular basis for peritoneal inflammation and tissue remodeling, we used two mouse models of postoperative and postinflammatory peritoneal adhesions. These models were used to study the traffic patterns of Mϕ in the peritoneal cavity. In this study, we describe a chemokine system that is specific for peritoneal Mϕ (PMϕ) but not bone marrow-derived Mϕ (BMϕ), a system that plays a significant role in both postoperative and postinflammatory peritoneal adhesion events.

Materials and Methods

Mice

Male 6- to 7-wk-old C57BL/6J mice obtained from CLEA Japan were maintained under pathogen-free conditions in a facility in the Research Institute, International Medical Center of Japan (IMCJ). Some experiment using *CCR8* gene-deficient ($CCR8^{-/-}$) mice of C57BL/6 background were performed using mice maintained under pathogen-free conditions in the facility of Okayama University. All experiments were performed according to the Institutional Guidelines for the Care and Use of Laboratory Animals in Research and with the approval of the local ethics committee.

Materials

Fluorescent nanocrystal quantum dots (QDs) (red emission) were produced as described previously (13, 14). Recombinant mouse CCL1 and MCP1 were purchased from R&D Systems. Rat anti-mouse CCL1 mAb and a control rat IgG were purchased from R&D Systems and The Jackson Laboratory, respectively. LPS from *Escherichia coli* O55B5 and peptidoglycan (PGN) from *Staphylococcus aureus* were purchased from Sigma-Aldrich and Fluka, respectively. Phosphorothioate-stabilized CpG oligodeoxynucleotide (5′-TCCATGACGTTCCTGATGCT-3′) was purchased from Takara Bio. Recombinant mouse TNF-α and IL-1β were purchased from PeproTech. For immunohistological examination, cryosections were stained with FITC-, PE-, or biotin-labeled anti-CD11b, anti-F4/80, anti-VLA4 (CD49a), and anti-Gr-1 mAbs (BD Pharmingen), rabbit anti-CCR8 polyclonal Ab (pAb; Abcam), and rabbit anti-mouse pan-cytokeratin pAb (Santa Cruz Biotechnology) followed by Alexa Fluor streptavidin (Invitrogen Life Technologies) or FITC-labeled goat anti-rabbit IgG pAb (Southern Biotechnology Associates).

Histological analysis

Tissues were snap-frozen and 6-μm sections were prepared and stained with H&E. For immunostaining, sections were fixed with cold acetone for 10 min, dried, and treated with Blockace (Dainippon Pharmaceuticals), incubated with indicated Abs followed by secondary Abs or fluorescent labeled streptavidin described in *Materials*. Images were captured with a fluorescence microscope (BX50/BXFLA; Olympus) equipped with a CCD camera. Merged images were produced using Adobe Photoshop CS2 (Adobe Systems).

Preparation of QD-labeled Mϕ and induction of postinflammatory and postoperative peritoneal adhesions

The cells collected from the peritoneal cavity were incubated in DMEM with 2% FCS for 45 min at 37°C on plastic dishes. After removal of the nonadherent cells by two washing steps, the adherent cells were gently scraped off with a silicon rubber scraper and used as naive PMϕ. Composition of this PMϕ preparation was constantly 92.9 ± 4.3% (mean ± 1 SD of four preparations) of CD11b-positive cells (granulocytes and Mϕ) and 87.5 ± 3.6% of F4/80-positive cells (Mϕ). The BMϕ were induced by M-CSF as described previously (15, 16). In some experiments, adherent PMϕ and BMϕ were incubated with QD solutions and labeled as reported previously (14), washed, and then scraped off. The labeling efficiency was 88%, and total cells were used for all experiments. We confirmed that the preparation and labeling process of PMϕ did not cause significant alteration in the expression of chemokine receptors, surface markers, and cell viability.

A model for postoperative peritoneal adhesions was created in mice as previously described (17). Briefly, a laparotomy was performed through a midline incision and two ischemic buttons were created on both sides of the parietal peritoneum by grasping the peritoneum with a hemostat clamp and ligating the base of the segment with a 4-0 silk suture. In some experiments, the QD-labeled PMϕ were injected i.p. after closing the abdominal wall. To induce colitis-associated peritoneal adhesions, a 2% solution of 2,4,6-trinitrobenzene sulfonic acid (TNBS; Research Organics)/ethanol 1:1 by volume was given rectally (4 μl/g body weight) (18). In some experiments, QD-labeled naive PMϕ were transferred by the i.p. routes 2 h before the induction of colitis.

Laser capture microdissection

Frozen sections were prepared from the colonic tissues with colitis and then stained with the HistoGene LCM Frozen Section Staining kit (Arcturus Bioscience) or anti-F4/80 mAb (BD Pharmingen). The $F4/80^{+}$ cells clustered at the serosal surface of the transmural ulcer of the colon were collected by use of the laser capture microdissection system (PixCell IIe LCM System; Arcturus Bioscience) to obtain an RNA fraction using the PicoPure RNA Isolation kit (Arcturus Bioscience).

RT-PCR

Total RNA isolated from cells and organs was subjected to RT-PCR. Primer structures are shown in Table I. Real-time quantitative PCR analysis was performed using a SYBR Green PCR Master Mix (Applied Biosystems) and the ABI 7700 Sequence Detector System (Applied Biosystems). Expression of mRNA was normalized to the levels of the GAPDH

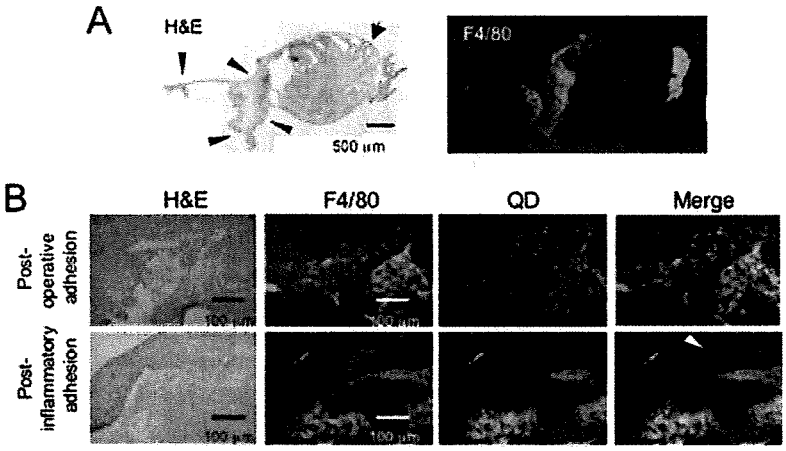

FIGURE 1. PMϕ form aggregates at the site of postoperative and postinflammatory peritoneal adhesions. *A*, Frozen sections prepared from peritoneal adhesions to ischemic buttons (postoperative model) were assessed. The serial sections were stained with H&E and with anti-F4/80 mAb. An arrow and arrowheads indicate the ischemic button and adhesive omentum, respectively. *B*, Frozen sections were prepared from peritoneal adhesions to ischemic buttons (postoperative model) or to the colon after induction of colitis (postinflammatory model) and subjected to H&E staining and immunostaining with anti-F4/80 mAb (green). The PMϕ (1×10^6) obtained from naive mice were labeled with QD (red) and i.p. transferred at the initiation of adhesions. Two images were overlaid in the merged image. Representative pictures from five mice in each experiment are shown. Bars represent 100 μm. Arrowhead indicates mucosal infiltration of Mϕ that does not contain QD-labeled PMϕ.

mRNA expressed. The step-cycle program was set for denaturing at 95°C for 15 s, annealing at 60°C, and extension at 72°C for 45 s, for a total of 40 cycles.

Chemotaxis assay

Aliquots of PMϕ or BMϕ (1×10^7 cells/ml) were prestained for 30 min at 37°C with 3 μg/ml 3′-*O*-Acetyl-2′,7′-bis(carboxyethyl)-4 or 5-carboxyfluorescein, diacetoxymethyl ester (Molecular Probes) and then suspended at 1×10^6 cells/ml in DMEM containing 0.5% BSA and 20 mM HEPES. A chemotaxis assay was performed using a Chemo Tx-96 Chemotaxis Plate (NeuroProbe), as follows. Pretreatment of cells was performed by incubation with or without 50 ng/ml CCL1 for 4 h. Enhanced expression of CCR8 in CCL1-treated PMϕ at this time point was confirmed by flow cytometry. After washing, 65 μl of cell suspension was loaded onto the membrane plate and placed onto a flat-bottom microtiter plate with 96 wells containing 30 μl of serially diluted CCL1 solution in each well. The plate was then incubated at 37°C for 90 min and cells which had undergone migration were collected. These collected cells were counted using a fluorescence microplate reader (FluoroScan Ascent FL; Labsystems). Some experiments were performed in the presence of pertussis toxin (PTX; Calbiochem).

ELISA for CCL1 secretion into peritoneal cavity

To determine the levels of CCL1 in the peritoneal cavity, we collected peritoneal lavage fluid. PBS (1.5 ml) was injected into the peritoneal cavity of mice with or without TNBS-induced colitis as described below, and 1.2–1.4 ml of fluid was recovered. After clearing by centrifugation, the level of CCL1 was determined using paired Abs (Ab Mab8451 for capture and biotinylated Ab BAF845 for detection; R&D Systems) according to the manufacturer's instructions. Bound Ab was detected with peroxidase-labeled avidin (Sigma-Aldrich) and tetramethyl benzidine was used as the substrate. Sensitivity of this assay was 0.2 ng/ml in our hands.

Chemokine-induced Mϕ aggregation (CIMA) assay

Mouse peritoneal mesothelial cells (PMCs) were isolated from omental tissue as described previously (19, 20). The PMCs (1×10^5 cells/well) were plated and cultured on the collagen-coated 24-well dish until they had reached confluence. The QD-labeled PMϕ were added to PMC cultures at a concentration of 1×10^5 cells/well in 10% FCS-DMEM. After addition of serial dilutions of CCL1 or other stimulants, the plates were incubated at 37°C and examined by fluorescent microscopy at the indicated time points. The formation of aggregates was quantified by capturing and analyzing images using NIH ImageJ (National Institutes of Health, Bethesda, MD). The cell aggregates which occurred in $>10\text{-}\mu m^2$ areas were picked and the total aggregation area in the field was summed. Three fields in each well were randomly chosen and analyzed.

Prevention of postinflammatory and postoperative peritoneal adhesions

In the colitis-associated adhesion model, anti-CCL1-neutralizing mAb or control rat IgG (150 μg) was administered 1 h before the colonic administration of TNBS. Mice were sacrificed at the indicated time point and the severity of adhesion was evaluated according to a standard scoring system reported previously (6) as follows: 0, no adhesion; 1, one thin filmy adhesion; 2, more than one thin adhesions; 3, thin adhesion with focal point: 4, thick adhesion with plantar attachment or more than one thick adhesion with focal point; 5, very thick vascularized adhesions of more than one plantar adhesion. In some experiments, the removed colon was observed with a Realtime In Vivo MacroImaging System (Relyon) equipped with long passed red-viewing filter (>610 nm wavelength) and a CCD camera (Hamamatsu Photonics). The area of fluorescent red color was extracted using Adobe Photoshop CS2 from captured images and quantified using ImageJ. In a model for postoperative peritoneal adhesions, 150 μg of anti-CCL1 mAb or control rat IgG was administered i.p. immediately after surgery and 3 days later. All mice were sacrificed at day 6 and the severity of adhesions to each ischemic button was scored according to the following system: 0, no adhesion; 1, thin filmy adhesion; and 2, thick planter adhesion.

Statistics

Data are expressed as mean ± SD. Statistical analysis was performed using the Statview II statistical program (Abacus Concepts) adapted for the Macintosh computer. The Student *t*, Tukey Kramer's honestly significant difference and Mann-Whitney *U* tests were used as indicated in the figure legends. Statistical interpretation of the results is indicated in the

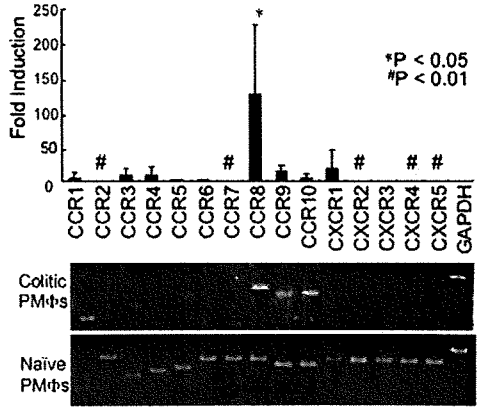

FIGURE 2. Expression of chemokine receptors in PMϕ aggregates at the adhesion after induction of TNBS colitis. Quantitative RT-PCR of cell aggregates obtained with laser capture microdissection from the F4/80$^+$ Mϕ aggregates 24 h after induction of TNBS colitis. Relative expression in aggregates was compared with naive PMϕ for each chemokine receptor as determined by quantitative RT-PCR. Results are shown as an average and 1 SD of four preparations of RNA samples obtained from each of four mice by microdissection. #*, Statistically significant up-regulation or down-regulation from PMϕ samples obtained from four naive mice by the Mann-Whitney *U* test, Representative pictures of PCR products are shown.

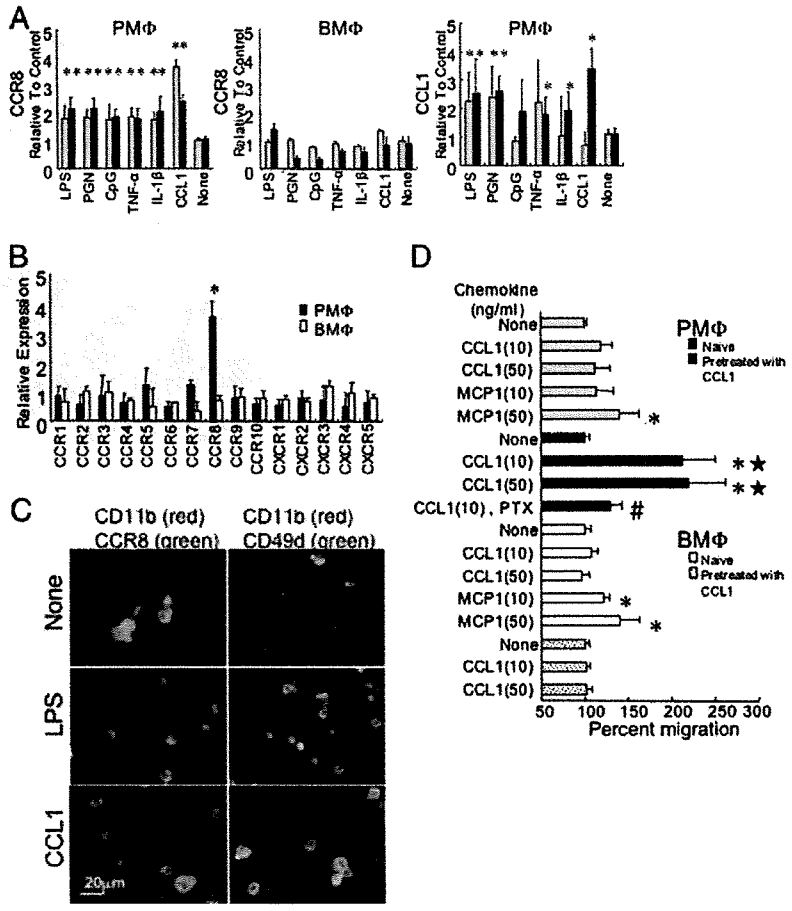

FIGURE 3. In vitro induction of CCR8 and CCL1 expression in PMϕ. *A*, Induction of CCR8 and CCL1 mRNA. PMϕ and BMϕ were stimulated with LPS (100 ng/ml), PGN (1 μg/ml), CpG (1 μg/ml), TNF-α (1 μg/ml), IL-1-β (10 μg/ml), or CCL1 (50 ng/ml) for either 2 (▨) or 4 h (■). Relative expression of mRNA to unstimulated cells was determined by quantitative RT-PCR and the results are shown as mean ± 1 SD of four to six independent cell preparations. *, The difference from unstimulated cells was statistically significant ($p < 0.01$) by the Mann-Whitney *U* test. *B*, Distinct induction of chemokine receptors in PMϕ and BMϕ by CCL1. PMϕ (■) and BMϕ (□) were stimulated with CCL1 (50 ng/ml) for 2 h and relative expression of chemokine receptor mRNA to unstimulated cells was determined by quantitative RT-PCR. Results are shown as mean ± 1 SD of four to six independent cell preparations. *, The difference from unstimulated cell preparations ($n = 6$) was statistically significant ($p < 0.01$) by the Mann-Whitney *U* test. *C*, Induction of surface expression of CCR8 in stimulated PMϕ. The PMϕ were incubated with 50 ng/ml CCL1 or 100 ng/ml LPS and stained with anti-CD11b mAb (red) to visualize the Mϕ cell membrane and with anti-CCR8 pAb (green) after 12 h or anti-CD49d mAb (green) after 48 h. *D*, Chemotaxis of PMϕ and BMϕ in response to CCL1. The PMϕ and BMϕ were pretreated with or without 50 ng/ml CCL1 for 4 h, washed, and subjected to the chemotaxis assay using CCL1 or MCP1 at indicated concentrations. ▨, PMϕ without pretreatment; ■, PMϕ pretreated with CCL1; □, BMϕ without pretreatment; ⊡, BMϕ pretreated with CCL1. Results were shown as mean ± 1 SD of three independent cell preparations. *, Differences from random migration without chemokine (MCP1(50) ▨ vs none ▨, CCL1(10/50) ■ vs none ■, and MCP1(10/50) □ vs none □) were statistically significant ($p < 0.01$); #, difference from chemotaxis without PTX (CCL1, PTX ■ vs CCL1(10/50) ■) was statistically significant ($p < 0.01$). ★, The difference from PMϕ without pretreatment (CCL1(10/50) ■ vs CCL1(10/50) ▨) or the difference from BMϕ (CCL1(10/50) ■ vs CCL1(10/50) ⊡) with the same pretreatment and chemokine concentration was statistically significant ($p < 0.01$). The statistical significance was determined by the Tukey Kramer's honestly significant difference test based on two-factorial ANOVA.

figure legends. Differences were considered statistically significant when $p < 0.05$.

Results

PMϕ trafficking in postoperative and postinflammatory peritoneal adhesions

We first used a postoperative peritoneal adhesion model where peritoneal ischemic buttons were induced by grasping and ligation of the parietal peritoneum. In this system, peritoneal adhesions were constantly formed within 6 days following the operation (17). Cells at the site of adhesion included neutrophils, $CD3^+$ lymphocytes, and $CD11c^+$ cells as reported previously (4–6); however, the infiltration of these cells was rather scattered. In contrast, we found that $F4/80^+$ PMϕ formed their own large aggregates (Fig. 1). In the TNBS hapten-induced colitis model, perforating colonic ulcers were constantly formed and always associated with the adhesions to adjacent tissue. We also found that adhesions to the colon were associated with the presence of Mϕ aggregates at the serosal side (Fig. 1*B*).

To investigate the possibility that PMϕ actually represent the source of these aggregating cells associated with peritoneal adhesions, we labeled naive PMϕ with fluorescent nanocrystal QDs and transplanted them into the peritoneal cavity of mice. QD-labeled PMϕ transferred to peritoneal cavity of naive mice resided in the omentum 24 h after transfer (data not shown). When QD-labeled PMϕ were transferred at the time of induction of postoperative or postinflammatory peritoneal adhesions, they accumulated in the cell aggregates at the serosal site of adhesions and perforating ulcers

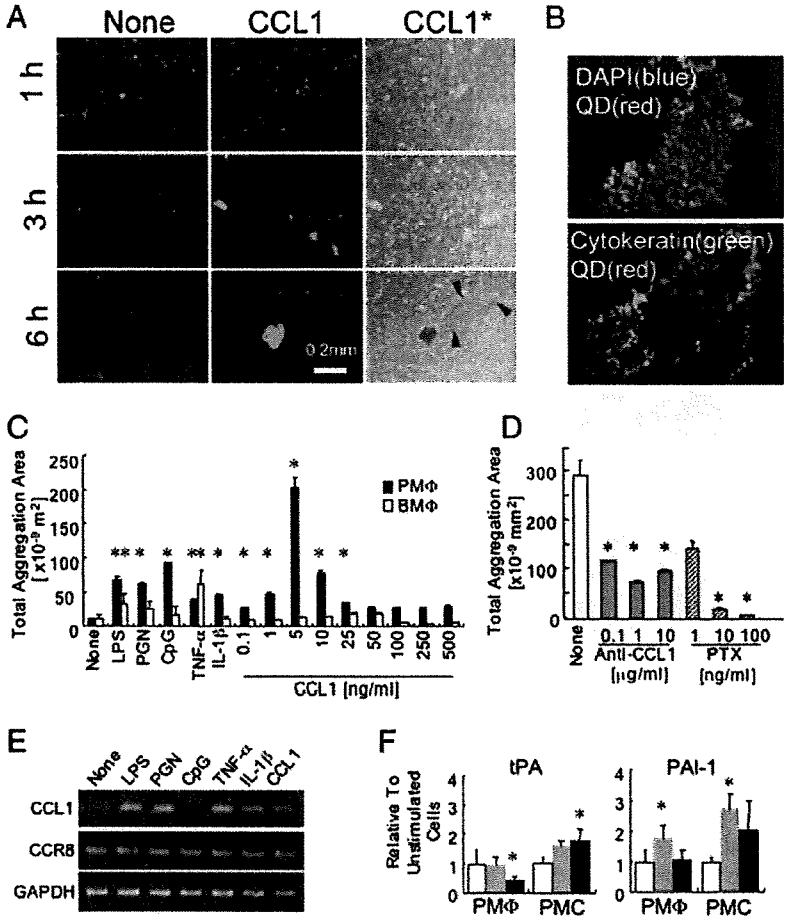

FIGURE 4. Chemokine-induced aggregate formation of PMϕ on monolayers of PMCs (CIMA assay). *A*, QD-labeled pooled PMϕ were placed on the PMC monolayer and stimulated with CCL1 (10 ng/ml) for 1, 3, and 6 h. Pictures are shown for one of three independent experiments with similar results. *, This column shows pictures taken under visible light, which were identical samples as the column using CCL1. Arrowheads indicate the traces of the detached PMC monolayer. *B*, Cell aggregates involve PMCs. The CCL1-induced, QD (red)-labeled PMϕ aggregates as in *A* were collected under a stereomicroscope after 24 h of incubation. Frozen sections were prepared and stained with 4,6 diamidino-2-phenylindole (DAPI, blue, *top*) or with anti-pancytokeratin Ab (green, *bottom*). Original magnification, ×400. *C*, Quantification of CIMA assays. The PMϕ (■) or BMϕ (□) were cultured on PMC monolayers with inflammatory stimulants at the concentrations described in the legend of Fig. 3*A* or at various concentrations of CCL1 for 24 h. The areas of aggregation in captured images were measured. Data are the mean aggregation area ± 1 SD of triplicate experiments. *, Statistically significant differences from cells without stimulation ($p < 0.01$) by the Student *t* test. *D*, Inhibitory effect of anti-CCL1-neutralizing mAb and PTX on aggregate formation. Coculture of PMϕ and PMCs was stimulated with 5 ng/ml CCL1 for 24 h in the presence of various concentrations of inhibitors. Data are the mean aggregation area ± 1 SD of triplicate experiments. *, The difference from controls (without anti-CCL1 mAb, blank column) were statistically significant ($p < 0.01$) by the Student's *t* test. *E*, Expression levels of CCL1 and CCR8 in PMCs after addition of proinflammatory stimuli or CCL1. The PMCs were incubated with stimulants at the concentrations described in the Fig. 3*A* legend or 50 ng/ml CCL1 for 6 h, and subjected to RT-PCR for CCL1 and CCR8. One representative result from four experiments, all giving an identical result, is shown. *F*, CCL1 altered expression of tPA and PAI-1. PMϕ and PMCs were left without stimulation (□) or stimulated with 50 ng/ml CCL1 for either 2 (▨) or 4 (■) h and subjected for quantitative RT-PCR. Results are the mean relative expression when compared with unstimulated cells ± 1 SD of six RNA preparations. *, Statistically significant difference from cells without stimulation ($p < 0.05$) by the Student *t* test.

(Fig. 1*B*). However, the cell infiltrates into the inflamed colonic wall hardly contained QD-labeled cells (Fig. 1*B*, arrowhead). These results indicated that peritoneal adhesions were associated with the massive recruitment of PMϕ to the serosal membrane.

Specific-induction chemokine receptors in PMϕ

To clarify the mechanism of aggregation of PMϕ, we next investigated the chemokine receptor expression patterns in PMϕ aggregates at the serosal surface of the inflamed colon using laser capture microdissection. In contrast to expression of mRNA for all chemokine receptors examined in naive PMϕ, aggregating F4/80$^+$ cells expressed only limited numbers of receptors, i.e., CCR8, CCR9, and CCR10 (Fig. 2). The results of real-time RT-PCR revealed that expression of mRNA for CCR8 was specifically high in aggregated cells (Fig. 2). Expression of CCR8 in serosal-aggregated PMϕ was also confirmed by immunohistological staining in both colitis and postoperative models (data not shown).

Up-regulation of CCR8 in PMϕ is induced by proinflammatory stimuli and by CCL1

We next investigated what types of stimuli might up-regulate mRNA for CCR8 in PMϕ. We found that significant up-regulation of CCR8 mRNA in PMϕ was induced by bacterial components, including LPS, PGN, and CpG, and by the proinflammatory cytokines TNF-α and IL-1-β (Fig. 3*A*). Notably, obvious up-regulation of CCR8 mRNA was induced by CCL1, the ligand for CCR8. In contrast, this degree of CCR8 mRNA up-regulation was not induced in BMϕ by any of stimuli tested (Fig. 3*A*). Up-regulation of

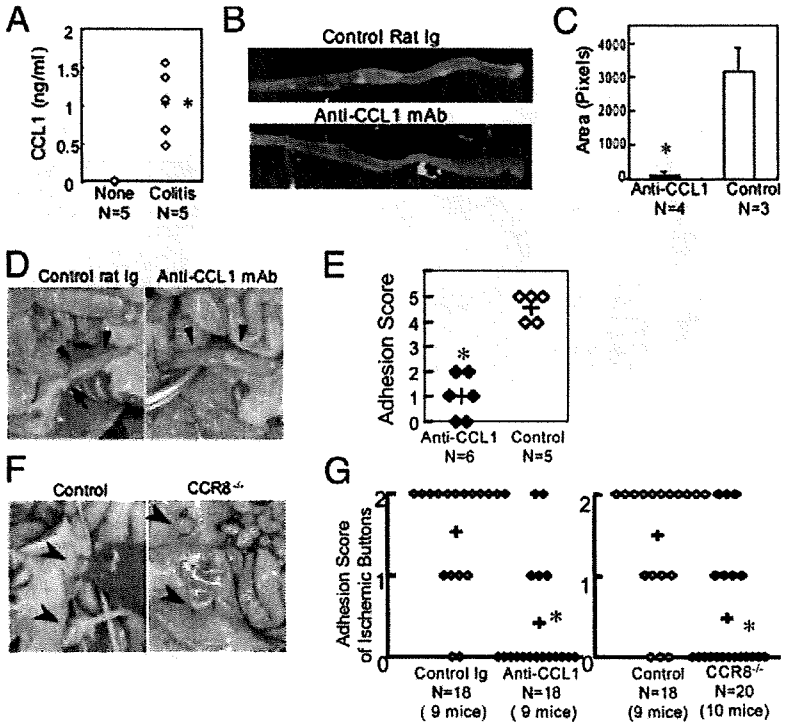

FIGURE 5. The anti-CCL1-neutralizing mAb prevented postinflammatory and postoperative peritoneal adhesions. *A*, Secretion of CCL1 in the peritoneal cavity after induction of colonic inflammation. Peritoneal lavage fluid obtained from naive mice or mice 24 h after induction of colitis with TNBS was subjected to CCL1 ELISA. CCL1 was below the detection limit (0.2 ng/ml) in all five naive mice. The difference was statistically significant ($p < 0.008$) by the Mann-Whitney *U* test, when the values from the naive mice were estimated as 0.2 ng/ml. *B*, Aliquots of QD-labeled (red) PMϕ (2.5×10^5 cells) were transferred to naive C57BL/6J mice on day −1. Next, rat anti-CCL1 mAb (150 μg) or the same amount of control rat IgG Ab were given i.p. and TNBS colitis was induced on day 0. Adhesive tissues in the colon were carefully cut and whole colonic tissues were obtained on day 1. Fluorescent images were superimposed to the pictures under visible light. Representative pictures from each group are shown. *C*, Quantification of QD-labeled cells migrated to the colonic surface. Red colored area in the fluorescent images as in *B* was measured. Results are shown as the mean ± 1 SD. *, Statistically significant difference from control mice ($p < 0.05$) by the Mann-Whitney *U* test. *D*, Anti-CCL1 mAb prevented postinflammatory peritoneal adhesions. Mice were given anti-CCL1 mAb (150 μg) or the same amount of control rat IgG 2 h before the induction of TNBS colitis. Four days later, peritoneal adhesion to the colon was assessed. Representative photos of the colon are shown. The arrows indicate multiple tissue adhesions to the colon in a control Ig-treated mice. Arrowheads indicate colon. *E*, Adhesion scores of mice treated with anti-CCL1 mAb. +, The average value. *, Statistically significant difference from control mice ($p < 0.01$) by the Mann-Whitney *U* test. *F*, Peritoneal adhesions to ischemic buttons were seen 6 days after the operation in control wild-type but not in CCR8$^{-/-}$ mice. The arrowheads indicate ischemic buttons. Typical thick planter adhesion to liver and omentum onto each ischemic button was seen in control mice, but not in CCR8$^{-/-}$ mice. *G*, Adhesion scores of postoperational adhesion in mice treated with control IgG or anti-CCL1 mAb (*left*). *Right panel*, Comparison of wild-type (control) and CCR8$^{-/-}$ mice. Adhesion score for each individual ischemic button was assessed. +, The average value. *, Statistically significant difference from control mice without stimulation ($p < 0.001$) by the Mann-Whitney *U* test.

CCL1 mRNA was also induced in PMϕ by LPS, PGN, TNF-α, IL-1β, and CCL1 itself (Fig. 3*A*). A 3-fold increase of CCL1 in PMϕ cultures stimulated with LPS was also detected by ELISA (data not shown).

Specific up-regulation of CCR8 in various chemokine receptors was seen in PMϕ treated with CCL1. In contrast, CCL1 did not induce particular chemokine receptors in BMϕ (Fig. 3*B*). Immunostaining for CCR8 after stimulation with CCL1 or LPS showed up-regulated expression of CCR8 in the PMϕ together with enhanced expression of the integrin CD49d (Fig. 3*C*), an adhesion molecule which had been reported to be expressed at the site of adhesions (21). Furthermore, we confirmed the function of CCL1-induced CCR8 in PMϕ using a chemotaxis assay. Pretreatment with CCL1 at the concentration of 50 ng/ml caused specific chemoattractive activity for PMϕ to CCL1. In contrast, the responses by BMϕ or untreated PMϕ to CCL1 were poor, although untreated BMϕ and PMϕ responded to MCP1 (Fig. 3*D*). CCL1-induced chemotaxis was inhibited by anti-CCL1 mAb as well as by PTX, which confirmed involvement of a G protein-coupled 7 transmembrane receptor such as CCR8 (Fig. 3*D*). Thus, under conditions where intestinal or peritoneal injury and inflammation occurs, there is a strong and specific positive feedback system to induce the CCL1/CCR8 chemokine system for the recruitment of PMϕ.

CIMA assay: an in vitro model for PMϕ aggregate formation and peritoneal adhesions

Our next experiments were directed to determine whether we could reconstitute aggregate formation of PMϕ associated with adhesions in vitro. When QD-labeled PMϕ were placed on a monolayer of mouse PMCs, PMϕ adhered to PMCs loosely and retained a rounded shape. Addition of CCL1 to this mixed culture led to formation of QD-positive cell aggregates with diameters of >100 μm by 3 h and at later time points (Fig. 4*A*). Importantly, the aggregates involved PMCs. The PMCs became detached from the culture plates and moved into the Mϕ cell aggregates to form a larger mass as shown by the presence of cells, which were QD negative but positively stained with an anti-cytokeratin pAb as a marker for PMCs (Fig. 4, *A* and *B*). Because the surface of the peritoneal cavity, including the omentum and viscera, are covered with mesothelial cells, this result suggests that organs and tissues could be pulled onto Mϕ aggregates via mesothelial cells to eventually form adhesions. In the absence of PMϕ, addition of CCL1

to the PMC layer did not induce detachment or morphological changes (data not shown). The PMϕ also formed aggregates in the presence of bacterial components including LPS, PGN, and CpG, and proinflammatory cytokines, TNF-α and IL-1-β (Fig. 4*C*). The optimal concentration of CCL1 for forming aggregates was ~5–10 ng/ml (Fig. 4*C*). This indicated that the concentration gradient of CCL1 made through this CCL1/CCR8 autocrine system of PMϕ was required for cell migration to form aggregates (Fig. 4*B*). At the high concentration in this one-chamber culture system, the concentration gradient around the cells would not be formed, even if cells produce CCL1. In contrast, BMϕ failed to form CCL1-induced aggregates on PMCs, although they responded to LPS and TNF-α to some extent (Fig. 4*C*). This CCL1-induced aggregate formation was significantly blocked by addition of anti-CCL1-neutralizing mAb or PTX (Fig. 4*D*). Because involvement of PMCs in the PMϕ aggregates was now established, we next investigated the responses of PMCs to CCL1. Although mRNA for CCL1 in unstimulated PMCs was hardly detected, LPS, PGN, TNF-α, IL-1β, and CCL1 induced dramatic up-regulation of CCL1 (Fig. 4*E*). CCR8 was constantly expressed on PMCs and expression level did not change with these stimuli (Fig. 4*E*). Thus, our in vitro model reproduced the initial steps in aggregate formation of PMϕ-enfolding PMCs and demonstrated that PMCs also facilitated the CCL1/CCR8-positive feedback system in PMϕ.

Furthermore, many studies have shown that early fibrinolytic events in the peritoneum play a central role in adhesion formation (1). To investigate possible involvement of CCL1 in the fibrinolytic pathway, mRNA levels for tissue-type plasminogen activator (tPA) and plasminogen activator inhibitor 1 (PAI-1) in the PMϕ and PMCs were assessed. Considerable levels of mRNA for tPA and PAI-1 were detected in unstimulated PMCs and PMϕ (data not shown). In PMϕ, expression of tPA was down-regulated, while that of PAI-1 was up-regulated 2 h after stimulation with CCL1 (Fig. 4*F*). In PMCs, significant up-regulation of PAI-1 was seen 2 h after starting treatment with CCL1 (Fig. 4*F*). Moderate up-regulation of tPA in PMCs became statistically significant when they were treated with CCL1 for 4 h. This CCL1-induced down-regulation of tPA in PMϕ and early up-regulation of PAI-1 in PMϕ and PMCs may also participate in the promotion of cell aggregation and adhesion formation.

Disruption of CCL1/CCR8 interaction prevents peritoneal adhesions

The establishment of a role for CCL1 in an in vitro model of cellular aggregate formation prompted us to investigate the effects of disruption of the CCL1/CCR8 system in vivo. Measurement of the levels of CCL1 in peritoneal lavage fluid revealed that CCL1 was significantly increased in mice with TNBS-induced colitis (Fig. 5*A*). Then, we found that the anti-CCL1-neutralizing mAb efficiently inhibited the formation of aggregates of QD-labeled PMϕ to the colonic serosa after induction of colitis (Fig. 5, *B* and *C*). Four days after induction of TNBS colitis, treatment with anti-CCL1 mAb caused less peritoneal adhesions when compared with mice treated with control rat IgG (Fig. 5, *D* and *E*). In our post-operative adhesion model, two ischemic buttons were created on both sides of the parietal peritoneum. Mice in the control group formed membranous thick adhesions to most of the ischemic buttons (Fig. 5*F*). In contrast, treatment with anti-CCL1 mAb efficiently reduced these adhesions (Fig. 5*G*). Frequency of adhesion formation in $CCR8^{-/-}$ mice was also decreased to the levels comparative to the mouse group treated with anti-CCL1 mAb (Fig. 5, *F* and *G*). Of note, blocking the CCL1-CCR8 interaction did not affect the healing of the initial operative incision.

Discussion

Little is known about cell trafficking between the peritoneal cavity and the organs of this locale including the gastrointestinal tract. We describe here for the first time the migration and aggregate formation of PMϕ at the site of injury. We have revealed the mechanism for this aggregate formation; a specific positive feedback system in PMϕ of the chemokine CCL1 and its receptor CCR8 when tissue damage or infection occurs. We have further established here an in vitro model for aggregation of PMϕ and PMCs, which was triggered by this same CCL1/CCR8 system. Finally, we were able to interrupt the migration of PMϕ and development of subsequent peritoneal adhesions by abrogating CCL1/CCR8 interaction. Each of these significant new findings is discussed in detail in the following paragraphs.

Practically no attention has been given to the serosal cell response in inflammatory disease of visceral organs. However, the damage and injury to viscera reaching the peritoneum is often fatal. In the case of murine colitis, we found that PMϕ form specific aggregates at the site of transmural ulcers and do not migrate into the inflamed colon. It is reasonable that these cell aggregates physically cover this tissue defect in the intestine and maintain a barrier to prevent further exposure to the flora, potential pathogens, or intoxicants. Apparently, the localization and function of PMϕ is distinct from other types of Mϕ, which are recruited directly from the bone marrow via the blood circulation and diffusely infiltrate into the mucosal and submucosal layer of the colon. This unique function of PMϕ is largely mediated through the restricted expression of a specific chemokine and its receptor. Naive PMϕ are responsive to many chemokines; however, PMϕ stimulated with CCL1 specifically up-regulate the expression of CCR8, which then facilitated the development of cell aggregates at this particular site of tissue damage.

The recruitment of PMϕ to the inflamed colonic serosa was dramatic. This was most probably explained by a specific and positive feedback system of CCL1/CCR8 in the PMϕ that we found here. In the case of transmural damage in the colon where normal flora reside, each stimulant positively induced up-regulation of the CCL1/CCR8 system in PMϕ. Because TNBS colitis induced in C57BL/6 mice was ameliorated by the administration of anti-CCL1 mAb (our unpublished data), there may be various inflammatory pathways downstream of CCL1 up-regulation. Previous reports showed that CCL1 functions as a migration inducer of Th2-type cells in both humans and mice (22, 23) as well as neutrophil Mϕ (24). Recent studies demonstrated that CCR8 was expressed in $CD4^+CD25^+$ T cells with IL-10 production (25) or FOXP3 expression (26). In addition, CCL1 was produced by a type of M2 (alternatively activated, M2b) Mϕ (27). Furthermore, rhadinovirus-transformed human T cells produced CCL1 with expression of CCR8, which supported cell growth and cytokine production (28). It is of interest that monocyte-derived dendritic cells use CCR8 in their migration to lymph nodes (29) and Langerhans-type dendritic cells in the skin also produced CCL1 when stimulated with various bacterial components (30). In humans, CCR8 is also expressed in vascular smooth muscle cells and mediates their chemotaxis (31). CCR8 was shown to play a significant role after bacterial challenge in the abdominal cavity in mice (32). However, autoinduction of the receptor CCR8, shown in our results, has not been clearly described to occur in any of these past studies. This vigorous autoactivation system is unique for PMϕ and may explain the rapid and massive recruitment of PMϕ into the injured viscera. This characteristic formation of aggregates by PMϕ certainly plays a key role in the immune system of the peritoneal cavity.

The reaction of PMϕ described here is a very effective defense system; however, in the case of surgical stress or chronic inflammation, we assumed that the reaction of PMϕ to serosal injury might represent a harmful mechanism that ultimately results in severe peritoneal adhesions. To address this notion, we first succeeded in the reconstruction of adhesions between PMϕ and PMCs in vitro. To our surprise, addition of only CCL1 to cocultures of PMCs and PMϕ induced the formation of large cell aggregates. Of interest, we found that mesothelial cells also showed striking up-regulation of CCL1 after various inflammatory conditions including incubation with CCL1 itself. When the intestinal damage reaches the serosal layer, mesothelial cells are exposed to bacterial components or inflammatory cytokines. At this point, CCL1 is first produced locally by mesothelial cells, where it initiates the recruitment and brisk activation of the CCL1/CCR8 system in PMϕ to support their migration and formation of cell aggregates. Furthermore, the enhanced expression of integrin molecules during the aggregate formation of PMϕ as well as up-regulation of PAI in PMCs and down-regulation of tPA in PMϕ via the CCL1/CCR8 system supports the significance of this chemokine system for promotion of further cell aggregation and adhesions, and finally for induction of firm fibrous adhesion tissue. Previous study described the role of T cells in the formation of adhesions (6, 7). Our experiment using T cell-deficient mice also indicated partial involvement of T cells in adhesion formation, however, CCL1-exposed PMϕ did not show enhanced production of TNF-α, IL-6, IL-4, or IL-10 (our unpublished data). The mechanism of the T cell activation along with the CCL1-driven PMϕ recruitment requires further investigation.

In the postoperative model, blockade of the CCL1/CCR8 interaction either with anti-CCL1 mAb or disruption of the *CCR8* gene decreased peritoneal adhesions, but did not affect the healing of the initial midline incision. This suggests a specific effect by blocking the CCL1/CCR8 interaction and points to the possible importance for use of CCL1/CCR8 antagonists to prevent postoperative adhesions without affecting wound healing. Currently, many clinical trials and experimental studies for prevention of peritoneal adhesions have been based upon the idea of modification of the fibrinolytic pathway (33) or the placement of chemical (34) or physical barriers (35, 36). Physical barrier placement was effective in preventing adhesions between viscera and the peritoneal wall; however, it failed to prevent adhesions between viscera. Antiadhesion treatments also includes antibiotics (37), the neurokinin 1 receptor antagonist (17), or cyclooxygenase-2 inhibitors (38, 39) which are mostly nonspecific anti-inflammatory regimen. In contrast, specific blocking of CCL1/CCR8 inhibited the aggregation of PMϕ but would not block the diffuse infiltration of BMϕ into the inflamed site, for the lack of CCR8. This feature suggests the advantage of targeting CCL1/CCR8 for prevention of adhesions, a procedure which would not affect mucosal or systemic defense systems or the wound healing process. Furthermore, we newly developed the CIMA assay in this study. It is now possible to select suitable molecules for use in prevention of peritoneal adhesions in combination of our CIMA assay and high throughput screening of CCR8 antagonists. We now provide a novel target to prevent excess inflammatory responses in the peritoneal cavity and also point to the possibility of prevention of postoperative peritoneal adhesions by blocking CCL1/CCR8 using Abs or antagonists.

Acknowledgment

We thank Dr. Tetsuya Hisoue at International Medical Center of Japan for advice on statistical analysis.

Disclosures

The authors have no financial conflict of interest.

References

1. Saed, G. M., and M. P. Diamond. 2004. Molecular characterization of postoperative adhesions: the adhesion phenotype. *J. Am. Assoc. Gynecol. Laparosc.* 11: 307–314.
2. Ellis, H., B. J. Moran, J. N. Thompson, M. C. Parker, M. S. Wilson, D. Menzies, A. McGuire, A. M. Lower, R. J. Hawthorn, F. O'Brien, et al. 1999. Adhesion-related hospital readmissions after abdominal and pelvic surgery: a retrospective cohort study. *Lancet* 353: 1476–1480.
3. Holmdahl, L. 1999. Making and covering of surgical footprints. *Lancet* 353: 1456–1457.
4. Ellis, H., W. Harrison, and T. B. Hugh. 1965. The healing of peritoneum under normal and pathological conditions. *Br. J. Surg.* 52: 471–476.
5. Haney, A. F. 2000. Identification of macrophages at the site of peritoneal injury: evidence supporting a direct role for peritoneal macrophages in healing injured peritoneum. *Fertil. Steril.* 73: 988–995.
6. Chung, D. R., T. Chitnis, R. J. Panzo, D. L. Kasper, M. H. Sayegh, and A. O. Tzianabos. 2002. CD4$^+$ T cells regulate surgical and postinfectious adhesion formation. *J. Exp. Med.* 195: 1471–1478.
7. Holsti, M. A., T. Chitnis, R. J. Panzo, R. T. Bronson, H. Yagita, M. H. Sayegh, and A. O. Tzianabos. 2004. Regulation of postsurgical fibrosis by the programmed death-1 inhibitory pathway. *J. Immunol.* 172: 5774–5781.
8. Rodgers, K. E., and G. S. diZerega. 1993. Function of peritoneal exudate cells after abdominal surgery. *J. Invest. Surg.* 6: 9–23.
9. Ar'Rajab, A., W. Mileski, J. T. Sentementes, P. Sikes, R. B. Harris, and I. J. Dawidson. 1996. The role of neutrophils in peritoneal adhesion formation. *J. Surg. Res.* 61: 143–146.
10. Day, D. W., J. R. Jass, A. B. Price, N. A. Shepherd, J. M. Sloan, I. C. Talbot, B. F. Warren, and G. T. Williams. 2003. Inflammatory disorders of the small intestine. In *Morson and Dawson's Gastrointestinal Pathology*, 4th Ed. Blackwell Science, Oxford, pp. 272–323.
11. Sheehan, A. L., B. F. Warren, M. W. Gear, and N. A. Shepherd. 1992. Fat-wrapping in Crohn's disease: pathological basis and relevance to surgical practice. *Br. J. Surg.* 79: 955–958.
12. Borley, N. R., N. J. Mortensen, D. P. Jewell, and B. F. Warren. 2000. The relationship between inflammatory and serosal connective tissue changes in ileal Crohn's disease: evidence for a possible causative link. *J. Pathol.* 190: 196–202.
13. Hoshino, A., K. Fujioka, T. Oku, S. Nakamura, M. Suga, Y. Yamaguchi, K. Suzuki, M. Yasuhara, and K. Yamamoto. 2004. Quantum dots targeted to the assigned organelle in living cells. *Microbiol. Immunol.* 48: 985–994.
14. Hoshino, A., K. Hanaki, K. Suzuki, and K. Yamamoto. 2004. Applications of T-lymphoma labeled with fluorescent quantum dots to cell tracing markers in mouse body. *Biochem. Biophys. Res. Commun.* 314: 46–53.
15. Lanotte, M., D. Metcalf, and T. M. Dexter. 1982. Production of monocyte/macrophage colony-stimulating factor by preadipocyte cell lines derived from murine marrow stroma. *J. Cell. Physiol.* 112: 123–127.
16. Merchav, S., and G. Wagemaker. 1984. Detection of murine bone marrow granulocyte/macrophage progenitor cells (GM-CFU) in serum-free cultures stimulated with purified M-CSF or GM-CSF. *Int. J. Cell Cloning* 2: 356–367.
17. Reed, K. L., A. B. Fruin, A. C. Gower, A. F. Stucchi, S. E. Leeman, and J. M. Becker. 2004. A neurokinin 1 receptor antagonist decreases postoperative peritoneal adhesion formation and increases peritoneal fibrinolytic activity. *Proc. Natl. Acad. Sci. USA* 101: 9115–9120.
18. Dohi, T., K. Fujihashi, H. Kiyono, C. O. Elson, and J. R. McGhee. 2000. Mice deficient in Th1- and Th2-type cytokines develop distinct forms of hapten-induced colitis. *Gastroenterology* 119: 724–733.
19. Bittinger, F., C. Schepp, C. Brochhausen, H. A. Lehr, M. Otto, H. Kohler, C. Skarke, S. Walgenbach, and C. J. Kirkpatrick. 1999. Remodeling of peritoneal-like structures by mesothelial cells: its role in peritoneal healing. *J. Surg. Res.* 82: 28–33.
20. Kato, S., Y. Yuzawa, N. Tsuboi, S. Maruyama, Y. Morita, T. Matasuguchi, and S. Matsuo. 2004. Endotoxin-induced chemokine expression in murine peritoneal mesothelial cells: the role of Toll-like receptor 4. *J. Am. Soc. Nephrol.* 15: 1289–1299.
21. Bellingan, G. J., P. Xu, H. Cooksley, H. Cauldwell, A. Shock, S. Bottoms, C. Haslett, S. E. Mutsaers, and G. J. Laurent. 2002. Adhesion molecule-dependent mechanisms regulate the rate of macrophage clearance during the resolution of peritoneal inflammation. *J. Exp. Med.* 196: 1515–1521.
22. Zingoni, A., H. Soto, J. A. Hedrick, A. Stoppacciaro, C. T. Storlazzi, F. Sinigaglia, D. D'Ambrosio, A. O'Garra, D. Robinson, M. Rocchi, et al. 1998. The chemokine receptor CCR8 is preferentially expressed in Th2 but not Th1 cells. *J. Immunol.* 161: 547–551.
23. D'Ambrosio, D., A. Iellem, R. Bonecchi, D. Mazzeo, S. Sozzani, A. Mantovani, and F. Sinigaglia. 1998. Selective up-regulation of chemokine receptors CCR4 and CCR8 upon activation of polarized human type 2 Th cells. *J. Immunol.* 161: 5111–5115.
24. Luo, Y., J. Laning, S. Devi, J. Mak, T. J. Schall, and M. E. Dorf. 1994. Biologic activities of the murine β-chemokine TCA3. *J. Immunol.* 153: 4616–4624.
25. Freeman, C. M., B. C. Chiu, V. R. Stolberg, J. Hu, K. Zeibecoglou, N. W. Lukacs, S. A. Lira, S. L. Kunkel, and S. W. Chensue. 2005. CCR8 is expressed by antigen-elicited, IL-10-producing CD4$^+$CD25$^+$ T cells, which regulate Th2-mediated granuloma formation in mice. *J. Immunol.* 174: 1962–1970.
26. Soler, D., T. R. Chapman, L. R. Poisson, L. Wang, J. Cote-Sierra, M. Ryan, A. McDonald, S. Badola, E. Fedyk, A. J. Coyle, et al. 2006. CCR8 expression

identifies CD4 memory T cells enriched for FOXP3$^+$ regulatory and Th2 effector lymphocytes. *J. Immunol.* 177: 6940–6951.
27. Sironi, M., F. O. Martinez, D. D'Ambrosio, M. Gattorno, N. Polentarutti, M. Locati, A. Gregorio, A. Iellem, M. A. Cassatella, J. Van Damme, et al. 2006. Differential regulation of chemokine production by Fcγ receptor engagement in human monocytes: association of CCL1 with a distinct form of M2 monocyte activation (M2b, type 2). *J. Leukocyte Biol.* 80: 342–349.
28. Tamguney, G., J. Van Snick, and H. Fickenscher. 2004. Autocrine stimulation of rhadinovirus-transformed T cells by the chemokine CCL1/I-309. *Oncogene* 23: 8475–8485.
29. Qu, C., E. W. Edwards, F. Tacke, V. Angeli, J. Llodra, G. Sanchez-Schmitz, A. Garin, N. S. Haque, W. Peters, N. van Rooijen, et al. 2004. Role of CCR8 and other chemokine pathways in the migration of monocyte-derived dendritic cells to lymph nodes. *J. Exp. Med.* 200: 1231–1241.
30. Gombert, M., M. C. Dieu-Nosjean, F. Winterberg, E. Bunemann, R. C. Kubitza, L. Da Cunha, A. Haahtela, S. Lehtimaki, A. Muller, J. Rieker, et al. 2005. CCL1-CCR8 interactions: an axis mediating the recruitment of T cells and Langerhans-type dendritic cells to sites of atopic skin inflammation. *J. Immunol.* 174: 5082–5091.
31. Haque, N. S., J. T. Fallon, J. J. Pan, M. B. Taubman, and P. C. Harpel. 2004. Chemokine receptor-8 (CCR8) mediates human vascular smooth muscle cell chemotaxis and metalloproteinase-2 secretion. *Blood* 103: 1296–1304.
32. Matsukawa, A., S. Kudoh, G. Sano, T. Maeda, T. Ito, N. W. Lukacs, C. M. Hogaboam, S. L. Kunkel, and S. A. Lira. 2006. Absence of CC chemokine receptor 8 enhances innate immunity during septic peritonitis. *FASEB J.* 20: 302–304.
33. Saed, G. M., and M. P. Diamond. 2003. Modulation of the expression of tissue plasminogen activator and its inhibitor by hypoxia in human peritoneal and adhesion fibroblasts. *Fertil. Steril.* 79: 164–168.
34. Yaacobi, Y., A. A. Israel, and E. P. Goldberg. 1993. Prevention of postoperative abdominal adhesions by tissue precoating with polymer solutions. *J. Surg. Res.* 55: 422–426.
35. Becker, J. M., M. T. Dayton, V. W. Fazio, D. E. Beck, S. J. Stryker, S. D. Wexner, B. G. Wolff, P. L. Roberts, L. E. Smith, S. A. Sweeney, and M. Moore. 1996. Prevention of postoperative abdominal adhesions by a sodium hyaluronate-based bioresorbable membrane: a prospective, randomized, double-blind multicenter study. *J. Am. Coll. Surg.* 183: 297–306.
36. Gago, L. A., G. M. Saed, S. Chauhan, E. F. Elhammady, and M. P. Diamond. 2003. Seprafilm (modified hyaluronic acid and carboxymethylcellulose) acts as a physical barrier. *Fertil. Steril.* 80: 612–616.
37. Oncel, M., N. Kurt, F. H. Remzi, S. S. Sensu, S. Vural, C. F. Gezen, T. G. Cincin, and E. Oleay. 2001. The effectiveness of systemic antibiotics in preventing postoperative, intraabdominal adhesions in an animal model. *J. Surg. Res.* 101: 52–55.
38. Katada, J., H. Saito, and A. Ohashi. 2005. Significance of cyclooxygenase-2 induced via p38 mitogen-activated protein kinase in mechanical stimulus-induced peritoneal adhesion in mice. *J. Pharmacol. Exp. Ther.* 313: 286–292.
39. Saed, G. M., A. R. Munkarah, and M. P. Diamond. 2003. Cyclooxygenase-2 is expressed in human fibroblasts isolated from intraperitoneal adhesions but not from normal peritoneal tissues. *Fertil. Steril.* 79: 1404–1408.

Dose-Dependent Differential Regulation of Cytokine Secretion from Macrophages by Fractalkine[1]

Noriko Mizutani,* Toshiharu Sakurai,† Takahiro Shibata,‡ Koji Uchida,‡ Jun Fujita,† Rei Kawashima,* Yuki I. Kawamura,*§ Noriko Toyama-Sorimachi,* Toshio Imai,¶ and Taeko Dohi[2]*§

Although expression of the fractalkine (CX3CL1, FKN) is enhanced in inflamed tissues, it is detected at steady state in various organs such as the intestine, and its receptor CX3CR1 is highly expressed in resident-type dendritic cells and macrophages. We hypothesized that FKN might regulate the inflammatory responses of these cells. Therefore, murine macrophages were pretreated with FKN and then stimulated with LPS. We found that macrophages pretreated with 0.03 nM FKN but not with 3 nM FKN secreted 50% less TNF-α than did cells treated with LPS alone. Cells treated with 0.03 nM FKN and LPS also showed reduced phosphorylation of ERK1/2 and reduced NF-κB p50 subunit. Interestingly, the p65 subunit of NF-κB was translocated to the nuclei but redistributed to the cytoplasm in the early phase by forming a complex with peroxisome proliferator-activated receptor (PPAR) γ. Exogenous 15-deoxy-Δ(12,14)-prostaglandin J2, a natural ligand for PPAR-γ, also induced redistribution of p65 with decreased TNF-α secretion after LPS challenge. Pretreatment with 0.03 nM but not 3 nM FKN increased the cellular levels of 15-deoxy-Δ(12,14)-prostaglandin J2 as well as mRNA of PPAR-γ. Requirement of PPAR-γ for the effect of 0.03 nM FKN was confirmed by small interfering RNA of PPAR-γ. In contrast, pretreatment with 3 nM FKN induced higher levels of IL-23 compared with cells pretreated with 0.03 nM FKN and produced TNF-α in a CX3CR1-dependent manner. These dose-dependent differential effects of FKN establish its novel role in immune homeostasis and inflammation. ***The Journal of Immunology,*** **2007, 179: 7478–7487.**

Fractalkine (CX3CL1, FKN[3]) is a unique chemokine produced as a membrane-bound molecule that consists of an intracellular tail, a short membrane-spanning region, and a glycosylated mucin-like stalk that extends from the cell surface holding the chemokine domain (1). FKN also exists as a soluble glycoprotein that is produced by proteolytic cleavage of the full-length molecule at a membrane-proximal site (2, 3). Expression of FKN in endothelial cells is induced by various inflammatory stimuli such as LPS, TNF-α, IL-1, and IFN-γ (4–6). Besides induction of chemotaxis, FKN also functions as an adhesion molecule to support leukocyte adhesion and transmigration (7, 8). A unique receptor for FKN, CX3CR1, is expressed abundantly by dendritic cells and macrophages/monocytes (9–11) as well as Th-type 1 cells, cytotoxic effector lymphocytes (12, 13), mast cells (14), neurons, astrocytes, and microglia (15–17). Since expression of FKN and expression of CX3CR1 can be induced by immune cells, studies have focused on the role of FKN as an inflammatory mediator. Indeed, FKN is up-regulated in the inflammatory site of rheumatoid arthritis (12, 18), inflammatory bowel disease (19), atherosclerosis (20), psoriasis (21), myositis (22), and various inflammatory conditions of the kidney (23) and brain (24), although FKN gene-disrupted mice did not show significant differences from wild-type mice in either steady-state or inflammatory conditions (25).

Conversely, studies using GFP/CX3CR1 knock-in mice have shown that a $CX3CR1^{high}CCR2^{-}Gr1^{-}$ subset of murine blood monocytes characterized by CX3CR1-dependent recruitment to noninflamed tissues and a short-lived $CX3CR1^{low}CCR2^{+}Gr1^{+}$ cell population is actively recruited to inflamed tissue (26). Furthermore, CX3CR1-positive dendritic cells are distributed abundantly in the lamina propria of the normal intestine (27). Recent studies have shown that circulating $CX3CR1^{+}CD117Lin^{-}$ precursors represent the origin of some subsets of resident macrophages and dendritic cells (28), and a small proportion of intestinal lymph dendritic cells are derived from $CX3CR1^{high}$ blood monocytes in vivo under steady-state conditions (29). These results indicated the role of the FKN/CX3CR1 system in homing of noninflammatory or resident subsets of dendritic cells and macrophages. Of interest, a considerable amount of FKN is produced by epithelial cells and other types of cells in the normal intestine (19, 30). In addition to its role in cell dynamics, we assumed that the physiological level of FKN in the intestine regulates the function of $CX3CR1^{+}$ macrophages. Resident macrophages in the normal intestine have the distinctive feature of hyporesponsiveness to various inflammatory stimuli, including bacterial components (31–33). This is in sharp contrast to circulating monocytes and splenic macrophages, which

*Department of Gastroenterology, Research Institute, International Medical Center of Japan, Tokyo, Japan; †Department of Clinical Molecular Biology, Faculty of Medicine, Kyoto University, Kyoto, Japan; ‡Laboratory of Food and Biodynamics, Graduate School of Bioagricultural Sciences, Nagoya University, Nagoya, Japan; and §Core Research for Engineering, Science, and Technology and ¶KAN Research Institute Inc., Kobe, Japan

Received for publication January 9, 2007. Accepted for publication September 25, 2007.

The costs of publication of this article were defrayed in part by the payment of page charges. This article must therefore be hereby marked *advertisement* in accordance with 18 U.S.C. Section 1734 solely to indicate this fact.

[1] This work was supported in part by grants and contracts from the Ministry of Health, Labour and Welfare, the Ministry of Education, Culture, Sports, Science and Technology, the Japan Health Sciences Foundation, Novartis Foundation (Japan) for the Promotion of Science, and the Mitsukoshi Health and Welfare Foundation.

[2] Address correspondence and reprint requests to Dr. Taeko Dohi, Department of Gastroenterology, Research Institute, International Medical Center of Japan, Toyama 1-21-1, Shinjuku, Tokyo, Japan. E-mail address: dohi@ri.imcj.go.jp

[3] Abbreviations used in this paper: FKN, fractalkine (CX3CL1); BMϕ, bone marrow-derived macrophage; 15d-PGJ_2, 15-deoxy-$\Delta^{12,14}$-prostaglandin J2; PPAR-γ, peroxisome proliferator-activated receptor γ; siRNA, small interfering RNA.

produce large amounts of proinflammatory cytokines in response to bacterial components. The inflammatory anergy of intestinal macrophages is thought to be important to maintain intestinal homeostasis. However, the mechanism by which macrophages acquire this feature is not yet fully understood. One important working hypothesis is that intestinal epithelial cells and stromal cells provide a particular microenvironment to promote inflammatory anergy, along with a variety of cytokines and chemokines as their products. Indeed, intestinal stromal cell-derived products downregulate both monocyte receptor expression and cytokine production (32). It is also likely that FKN participates in forming this microenvironment of the intestine to render macrophages immunologically hyporesponsive. Such anti-inflammatory activity of FKN has been reported previously. For example, FKN attenuated LPS-induced production of NO, IL-6, and TNF-α by rat (34) and mouse (17) microglia, which are phagocytotic cells and are responsible for cytokine production in the CNS. Pretreatment of rats with an anti-FKN Ab enhanced LPS-induced TNF-α levels in hippocampus and cerebrospinal fluid (35). However, the anti-inflammatory effect of FKN in bone marrow-derived or blood macrophages has not been documented.

In this study, we compared the effects of different concentrations of FKN on macrophages and found that relatively low concentrations of FKN suppressed LPS-induced TNF-α secretion by both bone marrow-derived macrophages (BMϕ) and the mouse macrophage cell line RAW264.7. We investigated the underlying mechanism and found for the first time that FKN induced the expression of both peroxisome proliferator-activated receptor (PPAR) γ and its ligand and altered the subunit usage of NF-κB after stimulation with LPS in macrophages, eventually decreasing the secretion of TNF-α. In contrast, higher concentrations of FKN, which may represent a local inflammatory condition, did not show such an immunosuppressive effect; instead, an up-regulation of IL-23 was seen.

Materials and Methods

Mice

Six- to 7-wk-old male C57BL/6J mice obtained from CLEA Japan and IL-10 knockout mice (C57BL/6J background; The Jackson Laboratory) were maintained under pathogen-free conditions in a facility of the Research Institute, International Medical Center of Japan (Tokyo, Japan). All experiments were performed according to the Institutional Guidelines for the Care and Use of Laboratory Animals in Research with the approval of the local ethics committee in the International Medical Center of Japan.

Histological immunostaining

Frozen sections were prepared from mouse intestine, fixed with cold acetone for 10 min, dried, and treated with Blockace (Dainippon Pharmaceuticals), incubated with hamster anti-FKN (22) or PE-labeled rat anti-F4/80 (Serotec) and rabbit anti-CX3CR1 (22), followed by secondary FITC-labeled anti-hamster IgG Ab (Southern Biotechnology Associates) or Alexa 488-labeled anti-rabbit IgG Ab (Invitrogen Life Technologies and Molecular Probes). Images were captured with a fluorescence microscope (BX50/BXFLA; Olympus) equipped with a CCD camera. Merged images were produced using Adobe Photoshop CS2 (Adobe Systems).

Cell culture, pretreatment with FKN, and stimulation with LPS

To obtain BMϕ, bone marrow cells were harvested and differentiated in DMEM containing 10 ng/ml M-CSF and 10% FBS for 7 days. RAW264.7 cells (American Type Culture Collection) were grown in DMEM supplemented with 10% FCS. Aliquots of 1×10^5 cells in 0.2 ml of culture medium were pretreated with the indicated concentration of recombinant mouse FKN (R&D Systems) for 12 h and then stimulated by addition of the indicated concentration of LPS (from *Salmonella minnesota*, L-2167; Sigma-Aldrich) to the culture. In some experiments, 15d-PGJ2 (Cayman Chemical) and mouse rIL-23 (R&D Systems) was added to the culture. To examine the effect of immobilized FKN, 96-well flat-bottom plates were coated with 0.1 ml of various concentrations of FKN in PBS for 12 h at 4°C. After washing with PBS, cells were placed and the culture was performed as above. Actual density of coated FKN after washing was not measured. The hamster anti-mouse FKN Ab for blocking FKN was prepared at KAN Research Institute (Kobe, Japan). To neutralize the effects of CX3CR1, purified rabbit anti-rat CX3CR1 polyclonal Ab (2 μg/ml; Torrey Pines Biolabs) was used with rabbit IgG (IBL) as a control. To neutralize the actions of IL-23, purified rat anti-mouse IL-23 p19 mAb (2 μg/ml; eBioscience) and purified rat IgG1 isotype control (BD Biosciences) were used as controls.

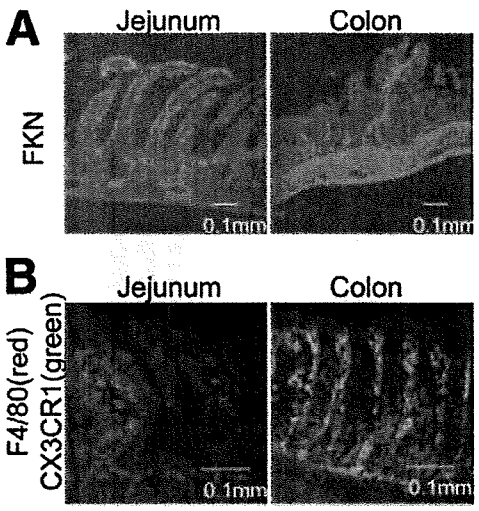

FIGURE 1. Expression of FKN in the intestine and detection of CX3CR1-positive macrophages. *A*, Frozen intestinal sections were stained with anti-FKN Ab. *B*, Frozen sections were double stained with anti-F4/80 (red) and anti-CX3CR1 Ab (green). Merged images are shown.

Cytokine production assay by ELISA

The concentrations of cytokines in culture supernatants were measured using a Murine TNF-α ELISA Development Kit (PeproTech), Quantikine M Mouse IL-6 Immunoassay kit (R&D Systems) and Mouse IL-10 ELISA kit (Endogen).

Flow cytometry analysis

Cells were incubated with mAb against mouse TLR4/MD-2 complex (SA15-21; a gift from Dr. S. Takamura-Akashi, Tokyo University, Tokyo, Japan) or isotype control IgG directly conjugated with Alexa 488 and analyzed by FACS (BD Biosciences).

Western blotting and immunoprecipitation

Cells were lysed in a buffer containing 150 mM NaCl, 50 mM Tris-Cl, 1 mM EDTA, 1 mM Na_3VO_4, 1 mM PMSF, 1% Nonidet P-40, complete protease inhibitor mixture (Roche Molecular Biochemicals), and 50 mM NaF (pH 8.0) for 20 min on ice. After centrifugation at 10,000 $\times$ *g* for 20 min, protein concentrations were determined using the Bio-Rad protein assay. After separation by SDS-PAGE under reducing conditions, lysates were transferred to membranes (Immobilon; Millipore) and subsequently immunoblotted with specific Ab before visualization by chemiluminescence (SuperSignal West Dura; Pierce). To analyze ERK1/2 activation, membranes were probed with anti-phospho ERK 1/2 Ab or total ERK1/2 Ab (Cell Signaling Technology) and then stripped and reprobed with Ab to actin (Santa Cruz Biotechnology). To detect the amount of NF-κB p50 protein, nuclear extracts were subjected to Western blotting with anti-NF-κB p50 Ab (sc-7178; Santa Cruz Biotechnology).

RT-PCR

Total RNA from cells was reverse-transcribed with Superscript II reverse transcriptase (Invitrogen Life Technologies) and amplified by PCR. The following primers were used; FKN, a forward primer (5′-CACCTCGGC ATGACGAAAT) and a reverse primer (5′-TTGTCCACCCGCTTCTC AA-3′); MD-2, a forward primer (5′-ATGTTGCCATTTATTCTCTTTT CGACG) and a reverse primer (ATTGACATCACGGCGGTGAATGA TG-3′); TLR4, a forward primer (5′-AGCAGAGGAGAAAGCATCTATG ATC) and a reverse primer (GGTTTAGGCCCCAGAGTTTTTCTCC-3′);